Environmental Earth Sciences (2023) 82:230
https://doi.org/10.1007/s12665-023-10897-0

THEMATIC ISSUE

Assessment of soil loss using RUSLE around Mongolian mining sites: a case study on soil erosion at the Baganuur lignite and Erdenet copper–molybdenum mines

Enkhjargal Sodnomdarjaa[1,2] · Frank Lehmkuhl[1] · Daniel Karthe[2,3,4] · Martin Knippertz[1] · Gantuya Ganbat[2]

Received: 1 April 2022 / Accepted: 6 April 2023 / Published online: 27 April 2023

Abstract

Mining constitutes an integral part of Mongolia's national economy and dominates the country's export revenue. At the same time, a wide range of mining impacts on soil, water resources, the atmosphere and the biosphere have been documented across the country. This case study addresses the long-term soil degradation around two mining sites located in the semi-arid steppe zone of Mongolia: the open-cast lignite mine of Baganuur about 140 km east of Ulaanbaatar, and the open-pit copper–molybdenum mine of Erdenet about 240 km northwest of Ulaanbaatar, both of which started commercial extraction in the late 1970s. For the assessment of soil erosion, the RUSLE model was applied in different seasons for the period from 1989 to 2018 at 3-year intervals, considering both climatic variation and the expansion of the mines based on maps and satellite imagery. Rainfall erosivity was identified as the most dominant factor driving soil erosion in the study regions, with mining leading to local increases in soil erodibility. The highest soil erosion rates were found in both areas in July 2018, reaching 7.88 t ha^{-1} $month^{-1}$ in the Erdenet area and 9.46 t ha^{-1} $month^{-1}$ in the Baganuur area. The spatial patterns of soil erosion showed higher soil loss rates were in the vicinity of the mines and adjoining industrial sites. Particularly high soil losses were identified in July 1998, July and August in 2013 and July 2018 in both mining areas. The combination of the RUSLE model, remote sensing and ground truth data as and their processing by GIS was found to be a time-saving and cost-effective technique for continuous monitoring of soil erosion and planning of preventive measures in and around mining areas.

Keywords Soil erosion · RUSLE · Erdenet mine · Baganuur mine · GIS

This article is part of a Topical Collection in Environmental Earth Sciences on ''The Soil-Water-Atmosphere Nexus'' guest-edited by Daniel Karthe, Lulu Zhang, Sabrina Kirschke, Nora Adam, Serena Caucci, and Edeltraud Günther.

✉ Enkhjargal Sodnomdarjaa
enkhjargal@gmit.edu.mn

1 Department of Geography, Chair of Physical Geography and Geoecology, RWTH Aachen University, Aachen, Germany

2 Engineering Faculty, German-Mongolian Institute for Resources and Technology (GMIT), Nalaikh, Ulaanbaatar, Mongolia

3 Institute for Integrated Management of Material Fluxes and of Resources, United Nations University, Dresden, Germany

4 Faculty of Environmental Sciences, Technische Universität Dresden, Dresden, Germany

Introduction

Over the past few decades, Mongolia's soils have been affected by a wide range of degradation phenomena including soil erosion, desertification, nutrient depletion and various forms of soil pollution (Batkhishig 2013; Hofmann et al. 2016; Han et al. 2021). Soil degradation in Mongolia is driven by the combined effects of climate change and anthropogenic activities including mining, (over-)grazing, agriculture, urbanization and offroad transportation (Lehmkuhl and Batkhishig 2003; Batkhishig 2013; Chonokhuu et al. 2019). About 72% of the country's land is considered to be degraded (Eckert et al. 2015; Darbalaeva et al. 2020; Liang et al. 2021) and the country has been facing severe desertification (Liang et al. 2021) which according to concerned scientists affects up to 90% of the total pastureland (Darbalaeva et al. 2020). Previously constrained to the regions bordering the Gobi desert, land degradation has in recent years increasingly affected the central part of Mongolia and to a lesser degree also extended to its north (Wang et al. 2020). The combined annual cost of land degradation in the country is estimated at around 2.1 billion USD or 43% of the country's GDP (UNCCD 2018). Batkhishig (2013) therefore noted, that an accurate estimation of soil erosion is crucial in Mongolia, but that there is limited knowledge regarding the spatiotemporal pattern of erosion and the distinction between predominant driving factors.

Over the past few decades, several scientific studies have been conducted on desertification and soil erosion in Mongolia. Climate change and anthropogenic land cover changes resulting from overgrazing, mining activities and deforestration have been documented as reasons for severe soil erosion and land degradation (Batkhishig 2013; Han et al. 2021; Liang et al. 2021). Studies based on remote sensing have recently provided an overview about soil erosion and desertification in Mongolia and identified mining activities as one of the major causes (Eckert et al. 2015). Large areas of land in Mongolia are adversely affected by mining activities, and around 4.6% of the territory of Mongolia currently covered by more than 2700 valid mining licenses (MRPAM 2020). There is well documented knowledge on mining related water, soil and air pollution in Mongolia (Knippertz 2005; Karthe et al. 2014, 2017; Timofeev et al. 2016; Chonokhuu et al. 2019; Kosheleva et al. 2018), but rather limited and case-specific documentation of mining impacts on soil erosion. Most previous studies have examined sediment transportation and soil erosion in agricultural areas, often combining field measurements and modelling approaches (e.g., Priess et al. 2015). Moreover, several studies have focused on the sources and impacts of sediments in Mongolian river system and identified high livestock densities along the rivers as the core challenge (e.g., Hartwig et al. 2016; Theuring et al. 2015). Onda et al. (2007) and Kato et al. (2010) measured soil erosion and sediment accumulation with radionuclide methods in the two small catchments of the Baganuur stream (0.076 km^2) and the Kherlen Bayan Ulaan stream (0.069 km^2). During the 2003 and 2004 monitoring period, annual soil erosion was estimated to be 0.37 t ha^{-1} $year^{-1}$ in Baganuur and 0.02 t ha^{-1} $year^{-1}$ in the Kherlen Bayan Ulaan, with precipitation playing the major role for sediment mobilization and suspended transport. Batkhishig et al. (2019) showed by the 137-Cesium radionuclide fallout method that the average soil erosion rate on a mean escarpment of the Ikh Bogd Mountains around Lake Orog was 12.57 ± 1.08 t ha^{-1} $year^{-1}$ and found a maximum soil erosion rate is 40.87 t ha^{-1} $year^{-1}$. This site is not impacted by mining, but its environment is comparable to the Erdenet and Baganuur mining sites but with steeper natural mountain slopes. Research into the causes of soil erosion has identified livestock and overgrazing as a main cause (Lehmkuhl and Batkhishig 2003) but also identified changing rainfall patterns and a trend toward strong convective rainfall events as a problem (Vandandorj et al. 2017).

Mining likely plays a significant but not sufficiently studied role for soil erosion in Mongolia. The country has more than 600 deposits of more than 80 types of minerals and ranks seventh in the world in terms of mineral resources (Davaasambuu 2018). The mining sector has been developing rapidly in recent decades and it is one of the country's most important sources of foreign direct investment (FDI), revenues and exports (Baatarzorig et al. 2018). For instance, in 2014–2016, the country's gross domestic product (GDP) increased by 1.2% due to decline in commodity prices and FDI in the mining sector. In 2017–2018, the GDP growth reached 5.3% due to a recovery of raw material prices and an FDI increase. This growth trend is expected to remain relatively stable in the future (Turmunkh 2020), averaging about 9% annually over the past decade (NSO 2018).

The economy in Mongolia is heavily dependent on the mining sector and revenues from mineral exports including particularly coal, gold and copper (Dagys et al. 2020). Although the rapid development of the mining sector is important for the country's economic development, it has been identified as an important driver of land degradation (Farrington et al. 2005). The effects of mining on water resources have been studied in some detail, including the sector's significant water in water-scarce regions, and the impacts of mining on ground and surface water pollution (Timofeev et al. 2016; Batbayar et al. 2017; Jarsjö et al. 2017; Nottebaum et al. 2020), and the challenges of aligning mining and water policies have recently been addressed (Schoderer et al. 2021). A few studies have investigated land degradation in major mining areas. The total damaged land area in the mining regions of the country was estimated at around 8.1 thousand hectare (ha) (Batmunkh 2021). Mining-related pollution has been linked to bioaccumulation by plants (Kosheleva et al. 2018) and several species of freshwater fish (Kaus et al. 2017), but also to a public health hazard (Nottebaum et al. 2020), thus pointing to a nexus of mineral extraction and the degradation of the abiotic and biotic environment.

In Mongolian mining areas, most previous work on soil degradation has focused on soil pollution, but little work has been done to assess mining-related erosion or to investigate the interlinkages between soil erosion and soil pollution. It has been reported that the generation of barren lands, mine tailings and stored overburdens has led to increased erosion particularly during the rainy season (Kayet et al. 2018). Some authors have described mining as growing concern regarding its role for land degradation (Khishigjargal et al. 2015) and observed a massive expansion of soil erosion due to mining (Batkhishig 2013). For the Tuul River Basin in Northern Mongolia, Jarsjö et al. (2017) applied the WATEM/SEDEM model to quantify the input of metal-contaminated sediments from Zaamar Goldfield mining area into the river system, and found the mining activities to strongly exacerbate natural soil erosion. The rate of soil loss around the Zaamar Goldfield mining area was reported to be 10 t km^{-2} $month^{-1}$, and the study found that mining-related soil losses contributed to pollutant transport in the mining area. In order to harmonize the development of mining sector in Mongolia with environmental sustainability, it is crucial to study and monitor environmental degradation and develop science-based environmental rehabilitation measures. This particularly includes soil losses due to erosion, which have not been investigated sufficiently in the past.

In this study, we aimed at the quantification and assessment of spatiotemporal pattern of soil erosion in two mining cities of Erdenet and Baganuur, with particular focus on the vicinity of the open-pit mining areas. For the time period from 1989 until 2018, we used a combination of terrestrial data and satellite-based information. The main objectives of this study were (1) to estimate soil erosion rate using the RUSLE method supported by Geographic Information Systems (GIS); (2) to classify spatiotemporal erosion risks and (3) to evaluate the spatial distribution in the two cities of Erdenet and Baganuur with particular focus on identifying the role of open-pit mining areas. The final results of the study can be used by decision-makers at the local, regional and national level to develop science-based soil erosion prevention and rehabilitation plans. This information is relevant both for mining officials and for government agencies responsible for the environmental oversight of mining operations.

Materials and methods

Study area

The objective of this study is to provide an integrated assessment of soil degradation at Mongolia's two largest open-pit mining sites: the Baganuur lignite mine and the Erdenet copper–molybdenum mining complex, both of which began commercial operation in 1978 (Fig. 1 and Table 1). Baganuur lignite mine is located in Baganuur district of Ulaanbaatar city (N 47°47′10″ E108°21′40″) and is 140 km east of the city center. The total district covers an area of 622 km^2, of which 416 km^2 is pastureland, 193 km^2 is settlement area, 0.047 km^2 belongs to the road and infrastructure network and 0.14 km^2 is governmental and other land. The city of Baganuur is home to a total population of 29,342 (NSO 2018). Baganuur district is located in a semi-arid steppe region at the Southern fringe of the Khentii Mountains, and the western bank of the Kherlen River which flows from north to south in the city's vicinity (Kim 2017). The district including mining sites is situated in a wide valley bounded by small hilly mountains in the west and east (Park et al. 2020). The mean annual temperature of Baganuur district is around—2.2 °C and the coldest month is January with an average temperature of—20.7 °C and the warmest month is July with an average temperature of + 18.2 °C (Climatedata 2020). The annual mean precipitation is around 250–280 mm and about 70% of the precipitation falls during the summer season from June to August (Kim 2017; Park et al. 2020). The territory of Baganuur area is filled with Cretaceous and Jurassic sediments with Quaternary alluvial, diluvial and aeolian sediments (Park et al. 2020). The Baganuur open lignite mine deposit was estimated at 812 million t in 2014 (Otgochuluu et al. 2015). Baganuur mining site has open pits, mining equipment and offices and the mine uses water through a municipal water supply system. Open-pit mining removes naturally vegetated areas and produces a high amount of waste that leads to an increase in soil pollution and soil erosion surrounding the area. Since the operation of Baganuur mining, 337 Mbcm overburden and 1100m^3/h groundwater usage were estimated (Park et al. 2020). The Erdenet Copper and Molybdenum complex is located in Erdenet city (N 49°03′38″ E104°03′31″) in Orkhon province, Northern Mongolia. Erdenet city was established in 1976 as a center of mining and industry, and it is the country's second-largest city. Orkhon province, which covers the two districts of Bayan-Undur (where the city of Erdenet is located) and Jargalant, encompasses a total area of 844 km^2, 464 km^2 of this are pasture land, 210 km^2 by settlement area, 9 km^2 by road and infrastructure, 2 km^2 by water bodies, and 140 km^2 by forest. The total population of Bayan-Undur district including Erdenet city is 101,909 (NSO 2018). The city is located in the Orkhon-Selenge volcanic sediment area, which consists of alkali-rich trachyandesite, granite intrusions and Carboniferous deposits (Battogtokh et al. 2013). The climate is continental with an average temperature of 0.7 °C and annual mean precipitation of 350 mm, the coldest month is January with an average temperature − 22.2 °C, and the warmest month is July with + 16.5 °C (Climatedata 2020) and 90% of total precipitation falls from May to September (Battogtokh et al. 2013). The city of Erdenet is located between two small streams, the Erdenet and the Gavil river, which merge into the Khangal river about 7 km downstream of the city in close proximity to the Cu Mo mine in the South and its large tailing pond in the North (Solongo et al. 2018). The Erdenet mine was established in 1978 and it is one of the largest copper and molybdenum mines in the world with metal deposits estimated as 7.6 Mt of copper (Cu) and 216 600 t of molybdenum (Mo) in 1991 (Munkhtsengel et al. 2006). The Erdenet open-pit mining complex consists of one tailings pond, dams, open-pit

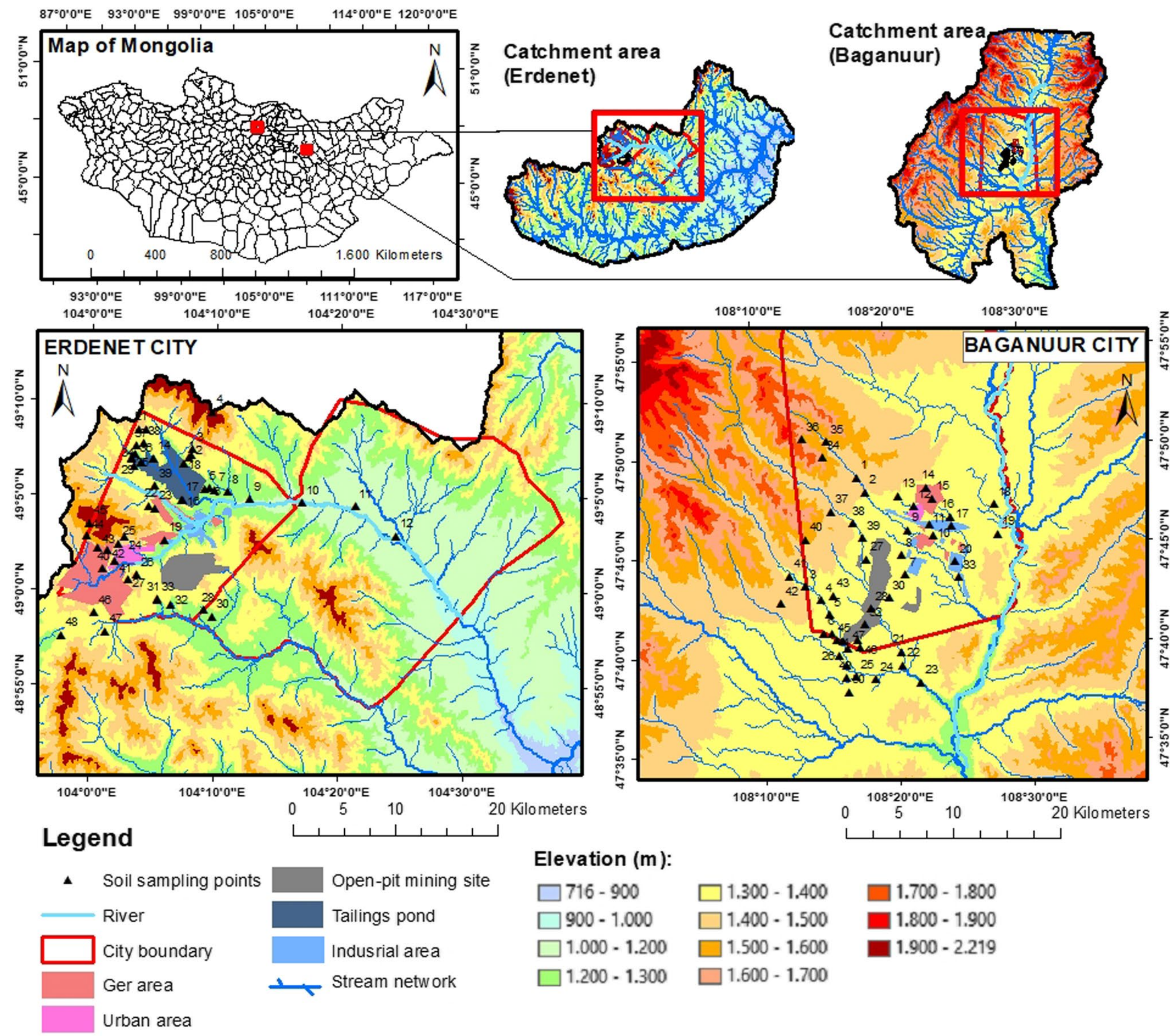

Fig. 1 Location of the study areas: Erdenet mining area in Erdenet city; Baganuur mining area in Baganuur city

Table 1 Key characteristics of the study area

Study area	Köppen–Geiger climate classification (Köppen 1936)	Average temperature (°C)			Annual mean precipitation (mm)	Elevation (m)	Mine site description (established year)
		Highest	Lowest	Mean			
Baganuur city	Semi-arid (steppe)	+ 18.2 °C (Jul)	− 20.7 °C (Jan)	− 2.2 °C	250–280	1150–2200	Baganuur lignite mine (1978)
Erdenet city	Continental and semi-arid (steppe)	+ 16.5 °C (Jul)	− 22.2 °C (Jan)	0.7 °C	350–400	700–2170	Erdenet copper–molybdenum (1978)

mines, a mine waste dump, and an ore processing mill complex. A locally well-known environmental impact of the mine is "white-dust", which is mobilized and transported by wind when parts of the tailings pond dessicate. White-dust affects soil and water quality around the tailings pond, which is problematic as this area is used by animals, herders, and residents to grow crops, and as it affects the Khangal River, which is a source of drinking and irrigation water (Battogtokh et al. 2013).

Data sources

In this study, the following data related to soil characteristics, land cover, topography and precipitation were collected to determine the spatio-temporal pattern of soil erosion.

Methods

Soil erosion estimation

In this study, the monthly soil erosion for the Baganuur and Erdenet mining areas was estimated using the Revised Universal Soil Loss Equation (RUSLE) model. It is based on the Universal Soil Loss Equation (USLE), which is considered a very practical approach that has been applied in more than 100 countries (Alewell et al. 2019). The USLE was developed in the late 1950s for assisting widespread application including soil conservation and soil management in a wide range of settings such as cropland, urban construction areas, recreational areas, and mine sites (Renard et al. 1991; USDA 2017). Due to some limitations of the original USLE method, the revised and updated USLE (RUSLE) was developed by Renard (1991). More recently, the application of remote sensing and GIS tools has become a standard practice for mapping soil erosion risks (Bahrawi et al. 2016). The RUSLE can easily combined with GIS and remote sensing approaches which can provide some of the input data (Kulimushi et al. 2021; see Table 2). Although the RUSLE model is widely used to estimate soil erosion worldwide, the model has been used in only a very few studies in Mongolia. The equation of the RUSLE model (Fig. 2) is based on (Schmidt et al. 2016, 2019):

$$A = R \times K \times LS \times C \times P, \quad (1)$$

where A is the quantification of soil loss in a month (t ha^{-1} year^{-1}), R is the rainfall erosivity factor (MJ mm ha^{-1} h^{-1} year^{-1}), K is the soil erodibility factor (t h MJ^{-1} mm^{-1}), LS is the topographic steepness factor (unitless), C is the cover management factor (unitless), P is the support and conservation practice factor (unitless) (Schmidt et al. 2016, 2019; Kebede et al. 2021). The annual soil loss equation was modified for calculating monthly soil loss using monthly based rainfall and vegetation data (Schmidt et al. 2019).

$$A_{\text{month}} = R_{\text{month}} \times K \times LS \times C_{\text{month}} \times P, \quad (2)$$

where A is the monthly soil loss in t ha^{-1} month.$^{-1}$

These input parameters are described in the following.

Rainfall erosivity factor (R)

The rainfall erosivity factor is one of the RUSLE input parameters that calculate precipitation and runoff impact on soil loss (Kayet et al. 2018; Lee et al. 2021). The amount

Table 2 Data description and source

In-situ data source, description	Inputs	Outputs
Top layer of the soil (0–10 cm) of the study sites (own data)	Soil data	Soil texture Soil organic matter content Soil erosion –K factor
Remote sensing data source, description	**Inputs**	**Outputs**
The United States Geological Survey: https://earthexplorer.usgs.gov/ Spatial resolution–30 m; Duration: July 1982 to October 2018	Landsat 4–5 data; Landsat 7, 8 data	Normalized Difference Vegetation Index (NDVI); Drought occurrence; Soil erosion: Land cover management factor – C factor
The United States Geological Survey: https://earthexplorer.usgs.gov/ Spatial resolution–30 m	Digital Elevation Model (DEM)	Soil erosion: Topographic steepness factor – LS
Global climate and weather data: https://www.worldclim.org/ Monthly precipitation, mm Spatial resolution–21 km^2	Precipitation data	Soil erosion: Rainfall intensity factor–R factor

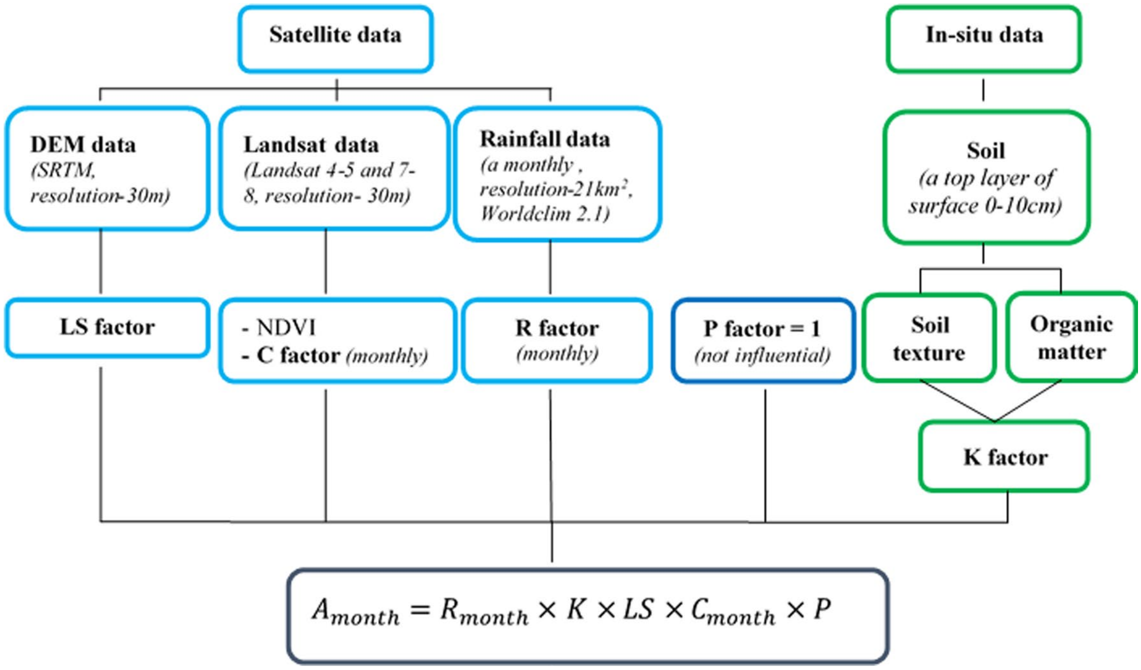

Fig. 2 The methodological framework of RUSLE model

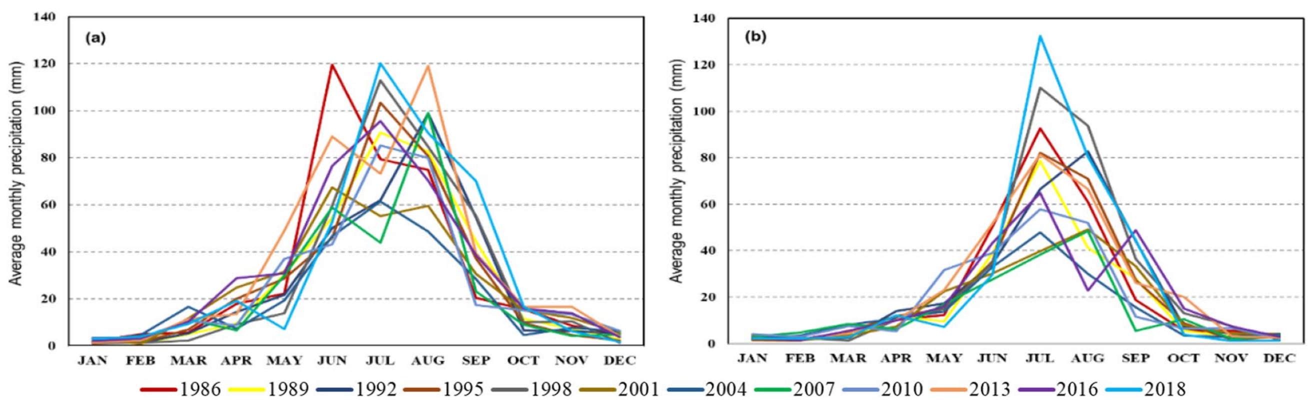

Fig. 3 Average monthly precipitation (mm) from 1986 to 2018 (Worlclim version 2.1 precipitation data for 1986–2018). **a** Erdenet, **b** Baganuur

of rainfall and its intensity is considered by this factor (Maqsoom et al. 2020). For calculation of the R factor, satellite-based Worldclim precipitation data (WorldClim) with a spatial resolution of 21 km^2 was used. For regions poorly covered by meteorological data, this database provides moderate spatial resolution data including long-term global monthly precipitation data (Abatzoglou et al. 2018). Average monthly precipitation around the two cities for 1986–2018 is shown (Fig. 3).

In this study, the monthly precipitation data of April to October from 1989 to 2018 were used in the calculation. The rainfall erosivity factor was calculated based on the following equation (Renard and Freimund 1994; Duulatov et al. 2021) based on monthly precipitation data. Rainfall point data were converted into raster data using the Inverse Distance Weighted (IDW) method in Arcmap software. The IDW method has been used for many studies to estimate R factor and it predicts the values in cells with unknown points (Ouadja et al. 2021).

$$R = 0.0483 + P^{1.61}, \tag{3}$$

where P is the monthly rainfall (mm). The rainfall data is satellite-based Worldclim precipitation data for 1989–2018.

Soil erodibility factor (K)

The soil erodibility factor (K) factor quantifies the relative susceptibility and transportability of soil from the surface due to rainplash and runoff (Kayet et al. 2018; Hateffard et al. 2021). The K factor is commonly classified based on soil texture and and soil organic matter content (Parveen and Kumar 2012), and ranges from 0.02 for the least erodible soil to 0.64 for the highest erodible soil (USDA 2017). A high amount of clay in soils has a high K value due to its easy erodibility, whereas loamy soil has moderate erodibility (Maqsoom et al. 2020). K factor values are negatively correlated with coarse textured soils and positively correlated with fine fractioned soils (Huang et al. 2022). In this study, the K factor was determined according to the soil texture type and soil organic matter content. The point data were converted into raster data using the Inverse distance weighted (IDW) method in Arcmap software. Soil samples were collected from the top layer of the surface (0–10 cm) inside and outside of the fences of the mining sites (Fig. 1). A total of 48 soil samples were collected from Erdenet mining sites in September 2020 and a total of 50 soil samples were collected from Baganuur mining sites in June 2020. Soil sampling points were georeferenced with a global positioning system (GPS Garmin 64) and are shown in Fig. 1. A total of 19 soil sampling locations were covered in a previous study by Knippertz (2005). Other sampling locations in Baganuur and Erdenet were selected randomly but represented different land covers including open-pit mining areas, urban and ger settlement areas, and the industrial zone. The simple random method was applied as it provides unbiased estimates of the mean and variance (Worsham et al 2012). In addition, it time saving and thus allows for a greater number of sampling points to be covered during the same time. All soil samples were air-dried under a normal air condition for 48 h in a laboratory of German-Mongolian Institute for Resources and Technology (GMIT) and sieved to less than 2 mm. The dry sieve method was used to determine the particle size fractions of the soil. In the process, 100 g of soil of each soil sample was subsequently placed in a sieves of 3 different diameters in order to classify it to fractions from 0.05 to 2.0 mm, 0.002 to 0.05 mm and < 0.002 mm according to USDA 2017. A shaking machine was used for 8 min with each sieve. Then the dry sieved results were used to determine soil textures based on a triangular diagram according to USDA standards.

The soil organic matter content of the samples was determined using the Loss on ignition (LOI) method. This method is one of the most commonly used methods for estimating soil organic matter content (Heiri et al. 2001). The soil samples were air dried at 22–25 °C for 48 h and particle larger than 2 mm were removed. Then, 5.00 ± 0.01 g of soil from each sample was oven dried for 24 h at 105 °C. After that, the dried samples were cooled in a desiccator, then the samples were heated at 360 °C for 2 h and then cooled below 105 °C (Schulte and Hopkins 1996).

Table 3 Soil erodibility factor relationship between Soil Organic Matter Content (SOM) (Schwab et al 1981)

Soil texture	Amount of organic matter (%)		
	0.5	2.0	4.0
Silty clay	0.25	0.23	0.19
Fine sand	0.16	0.14	0.1
Silt clay loam	0.37	0.32	0.26
Very fine sand	0.42	0.36	0.28
Clay loam	0.28	0.25	0.21
Loamy sand	0.12	0.10	0.08
Silt loam	0.78	0.42	0.33
Loamy very fine sand	0.44	0.38	0.30
Sandy loam	0.27	0.24	0.19

$$\mathrm{SOM} = \frac{\left(S_{w1} - S_{w2}\right)}{S_{w1}} \times 100, \tag{4}$$

where S_{w1} is the soil weight after drying at 105 °C, S_{w2} is the soil weight after heating 360 °C. The soil erodibility factor was then estimated based on texture and soil organic matter content (see Table 3).

Topographic steepness factor (LS)

Topographic steepness factor (LS) is used to estimate the impact of topography on soil erosion. Soil loss amount per area is directly correlated with the length of the slope (Tessema et al. 2020). The higher and lower slope has high risk of soil erosion (Kayet et al. 2018). It can be estimated by field measurement or a Digital Elevation Model (DEM) with GIS (Maqsoom et al. 2020; Kayet et al. 2018; Hateffard et al. 2021). In this study, satellite-based DEM data (Fig. 1) from the Shuttle Radar Topography Mission (SRTM) was obtained from the U.S Geological Survey's web site (USGS). The spatial resolution of the SRTM DEM data is 30 m, and its vertical resolution is 16 m or better (Mukul et al. 2017). In this study, the following equation was used to calculate the topographic steepness factor (Parveen and Kumar. 2012; Hateffard et al. 2021).

$$\mathrm{LS} = \left(\chi \times \frac{\lambda}{22.13}\right)^{0.5} \times (\mathrm{Sin}\beta/0.0896)^{1.3}, \tag{5}$$

where χ is the flow accumulation, λ is the raster cell dimension, β is the slope inclination in degrees (∘).

Land cover and management factor (C)

The land cover and management factor (C) is used to estimate soil loss from an area of a particular vegetation cover. Besides soil properties and slope steepness, the C factor is one of the most important drivers of soil erodibility (Panagos et al. 2015). Vegetation cover protects the soil surface from the impact of raindrops, and reduces runoff velocity, and even partial vegetation cover significantly reduces soil erosion (Boussaadi and Mauzai 2021). In this study, the C factor was calculated based on the Normalized Difference Vegetation Index (NDVI) using the equation (Durigon et al. 2014) below.

$$C = 0.1 \times \left(\frac{-NDVI + 1}{2} \right). \tag{6}$$

The NDVI is one of the vegetation indices, that estimates the amount of green vegetation cover in a particular landscape. It ranges from − 1.0 for to 1.0, where higher values represent higher vegetation cover and lower values represent low vegetation cover or barren land surface. In this study, NDVIs for the years 1989 to 2018 were presented as seasonal information in the following way: spring (April to May), summer (June to August) and autumn (September to October). This corresponds with the typical definition of these seasons in Mongolia (where the period from November to March can be considered as winter). Only, cloud-free or nearly cloud-free Landsat images were selected (Land cloud cover (LCC) ≤ 10%) and downloaded (via USGS) calculating the NDVI.

$$\mathrm{NDVI}_{L4-7} = \left(\frac{(B4 - B3)}{(B4 + B3)} \right), \tag{7}$$

$$\mathrm{NDVI}_{L8} = \left(\frac{(B5 - B4)}{(B5 + B4)} \right). \tag{8}$$

Conservation factor (P)

The conservation factor (P) represents the effect of precautionary measures for reducing soil erosion rate such as land treatments of countering, compaction, and constructive measures to control runoff and sediment transport (Maqsoom et al. 2020). It ranges from 0 for high-quality preservation practice to 1 for poor protection practices (Kayet et al. 2018). In this study, the P factor for the whole area of both cities was set as 1 (not influential) to calculate the RUSLE model as no prevention practices were applied in the two regions, except for limited drainage systems in the urban area around both mining regions.

Soil erosion risk

Spatial patterns of soil erosion rates were visualized based on classification steps of 0–0.1, 0.1–0.5, 0.5–1, 1–2, 2–3, 3–5 and > 5 t ha^{-1} $month^{-1}$ for showing lower to higher erosion rates regarding to Schmidt et al. 2016.

Results

R factor estimation

The average monthly value of the R factor from April to October for 1989–2018 ranges from 43.7 to 63.36 MJ mm h^{-1} $month^{-1}$ in Erdenet area and from 34.46 MJ mm h^{-1} $month^{-1}$ to 42.86 MJ mm h^{-1} $month^{-1}$ in the Baganuur area. Generally, the average monthly rainfall erosivity factor was higher in Erdenet area than in the Baganuur area due to higher rainfall in Erdenet.

Moreover, the highest average monthly rainfall erosivity factor was found during the vegetation growing season (June to August) in both study areas, ranging from 112.91 to 156.84 MJ mm h^{-1} $month^{-1}$ in Erdenet and from 95.43 to 112.41 MJ mm h^{-1} $month^{-1}$ in Baganuur (Table 4).

C factor estimation

The values of the C factors in the two mining areas differ according to the density of vegetation cover. Average C values range from 0.02 to 0.073 around Erdenet city and from 0.03 to 0.068 around Baganuur city during the period from 1989 to 2018 (Table 5). The value of the C factor were higher in the vicinity of the tailings pond and open-pit in both mining areas (Fig. 4) indicating higher vulnerability to erosion. The C factor decreased around both mining area in the growing season, which corresponds to the season of highest precipitation across Mongolia.

When rainfall was identified the dominant cause of temporal variations in soil erosion, the C factor based on the vegetation index NDVI was identified as a good predictor of spatial erosion pattern. On the one hand, the C factor reflects the seasonal pattern of vegetation growth. On the other hand, it clearly identifies barren lands that are a consequence of mining operations. The map of spatial distribution of NDVI is shown in Fig. 5 and Fig. 6 to show the difference between the highest and lowest precipitation during the peak season of vegetation cover (June to August) during the study period 1989–2018 in both areas.

Table 4 Average R factor (MJ mm h^{-1} $month^{-1}$) in different months during the study period from 1989 to 2018

Study areas	Average: Apr–May		Average: June–Aug		Average: Sep–Oct		Average: Apr–Oct	
	Lowest	Highest	Lowest	Highest	Lowest	Highest	Lowest	Highest
Erdenet	5.01	12.95	112.91	156.84	10.12	15.96	43.7	63.35
Baganuur	6.41	11.55	95.43	112.41	7.07	10.94	34.45	42.86

Table 5 Average C factor in different months

Study areas	Average: Apr–May		Average: June–Aug		Average: Sep–Oct		Average: Apr–Oct	
	Lowest	Highest	Lowest	Highest	Lowest	Highest	Lowest	Highest
Erdenet	0.036	0.07	0.013	0.067	0.026	0.072	0.025	0.07
Baganuur	0.034	0.06	0.017	0.072	0.035	0.074	0.029	0.071

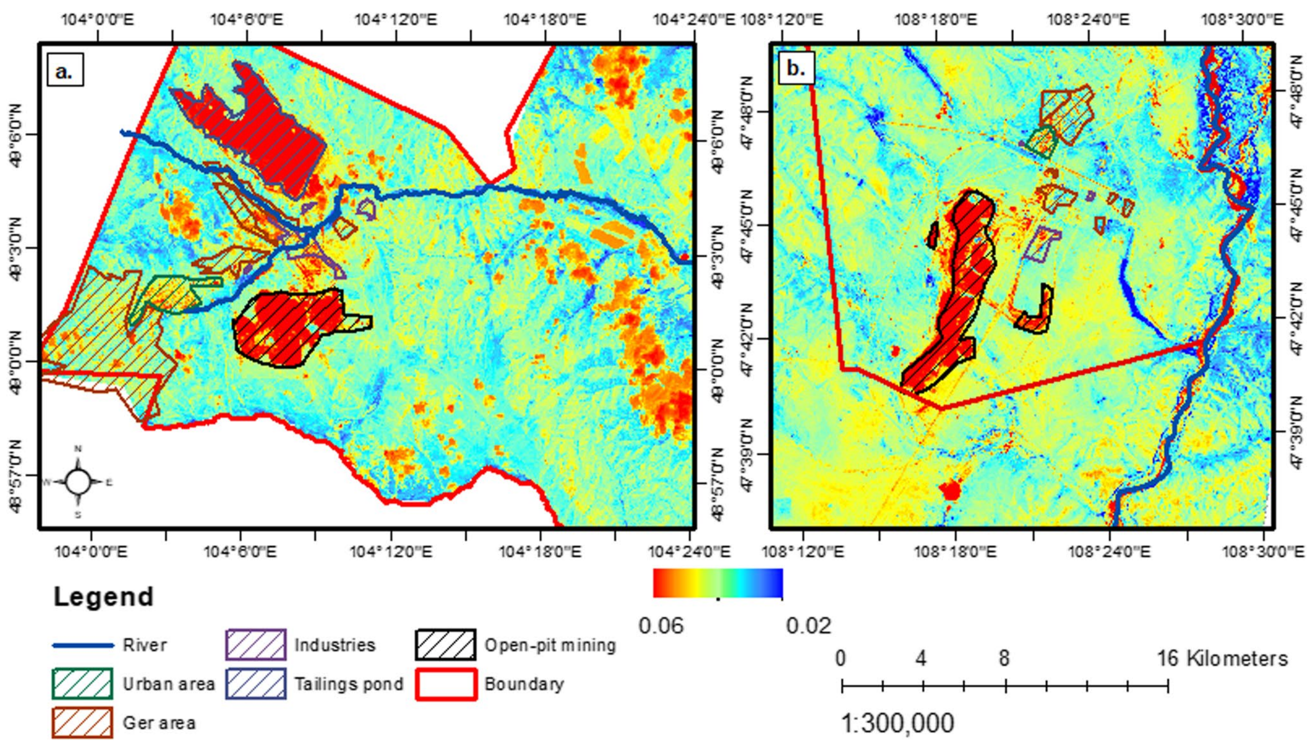

Fig. 4 Spatial pattern of the C factor around two mining areas: **a** Erdenet, **b** Baganuur

The spatial patterns of NDVI in wet and dry month and years clearly show that vegetation cover increases when precipitation is higher. However, the results of soil erosion showed that soil erosion rate during the study period was higher in the peak vegetation season from June to August and lower in autumn and spring. Rainfall amount is the most important factor in increasing soil erosion rate. This result is consistent with previous studies (Vandandorj et al. 2017; Schimdt et al. 2019; Shojaei et al. 2020; Duulatov et al. 2021).

K factor estimation

The soil erodibility factor was defined based on SOM content and soil texture. The estimated organic matter content in Erdenet area was 0.16–0.41% and in Baganuur area

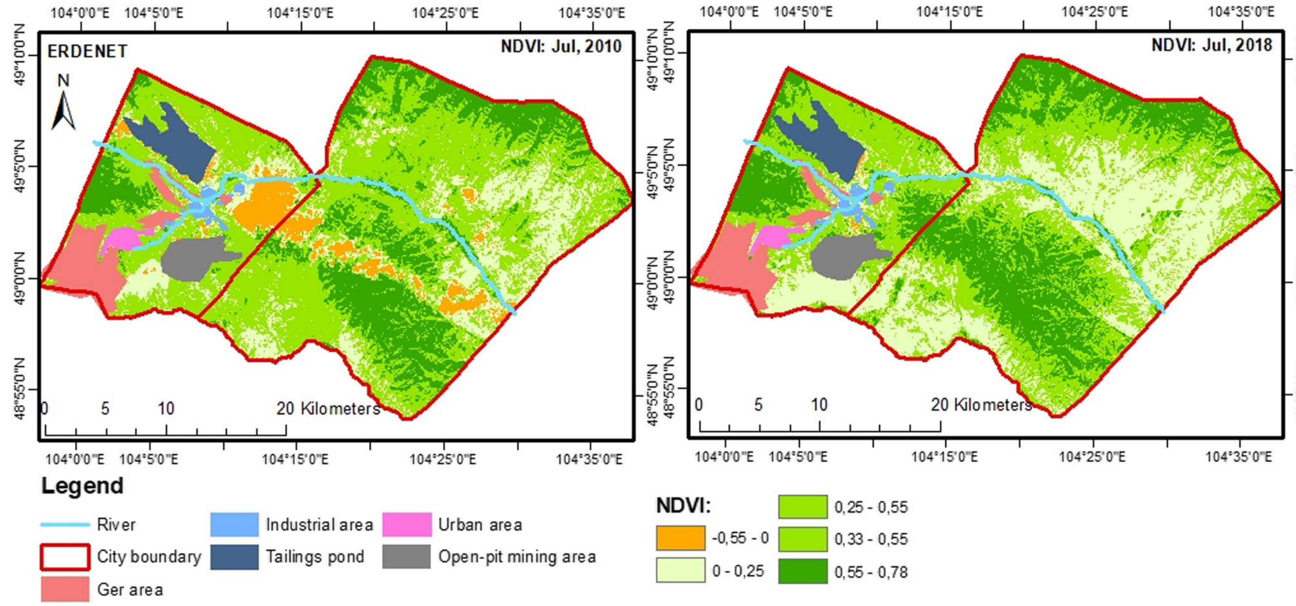

Fig. 5 Spatial patterns of NDVI regarding the highest and the lowest rainfall months during the study period in higher vegetation higher vegetation cover season in Erdenet area (The lowest: Jul 2010. The highest: Jul 2018)

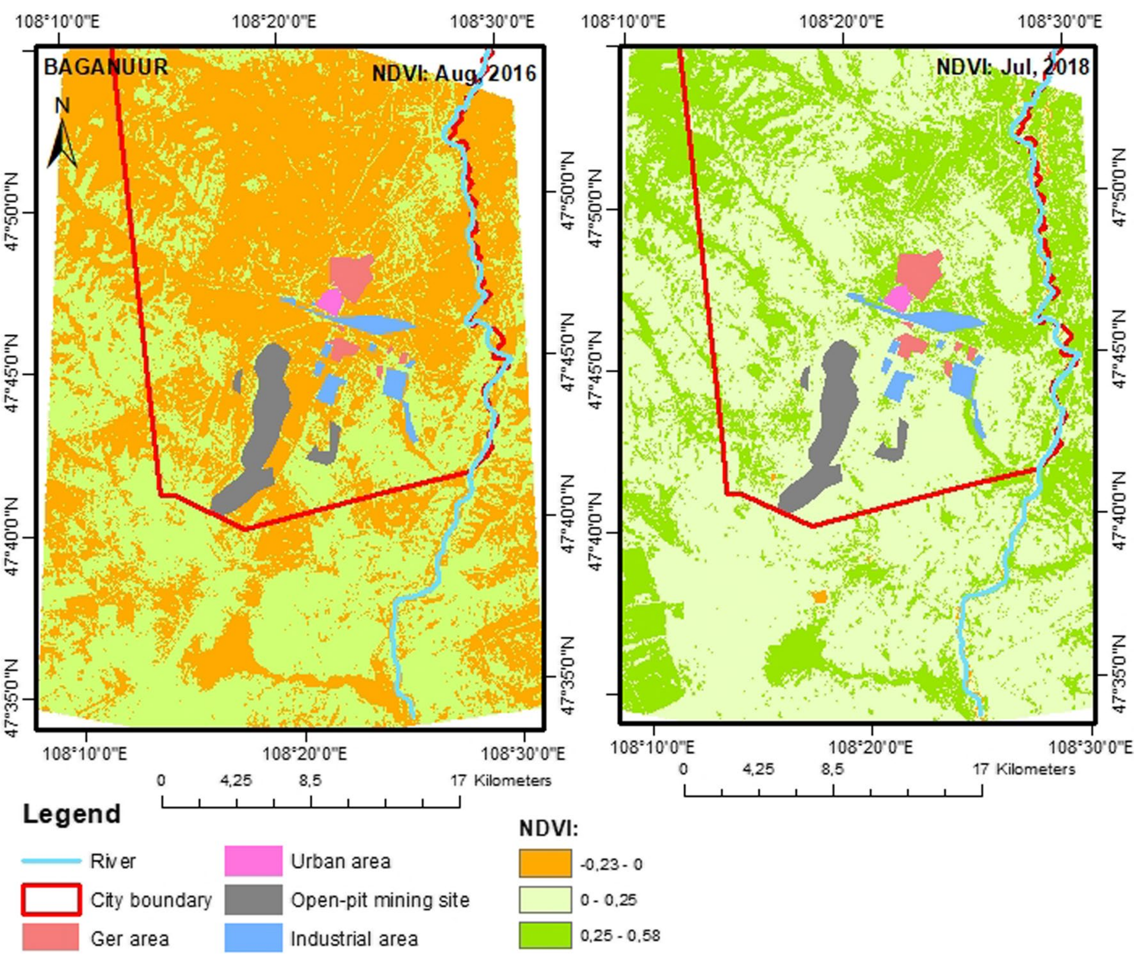

Fig. 6 Spatial patterns of NDVI regarding the highest and the lowest rainfall months during the study period in higher vegetation cover season in Baganuur area (The lowest: Aug 2016. The highest: Jul 2018)

0.05–0.36%. The soil textures of the sampled soils were generally sandy soil (92% of the total samples in Erdenet and 94% in Baganuur), with some loamy and sandy loam textures in the Erdenet area, and loamy sand and sandy loam textures found in Baganuur. These findings agree with literature which describes the soils of Baganuur as sands consisting of quartz, albite and microline (Park et al. 2020), and fine sand and some silt as the predominant soil textures around Erdenet (Battogtokh et al. 2013). Regarding to the SOM content and soil texture, the K values were selected from Table 3 as 0.12-loamy sand; 0.25-sandy loam; 0.27-sandy soil. The spatial patterns of the K factor were created in ArcMap software using the IDW technique.

LS factor estimation

The LS factor describes the combined effects of slope gradient and slope length (Maqsoom et al. 2020). In this study, the LS factor was calculated using Digital Elevation Model (DEM) data. The results of the LS factor ranged from 0 to 9.6 around the Erdenet mining area and 0–5.7 around the Baganuur mining area. In both areas, higher values of the LS factor were observed at higher altitudes due to longer and steeper slopes (Duulatov et al. 2021).

Assessing soil erosion for 1989 to 2018

The average monthly soil erosion rate was calculated in three different seasons: for spring (April to May), for summer (June to August), and for autumn (September to October) (Table 6). The average soil erosion rate was higher in Erdenet area than in Baganuur area due to higher rainfall in Erdenet.

The results of soil erosion modelling from 1989 to 2018 show that both study areas are susceptible to soil erosion, especially during periods of higher precipitation. Previous studies have found that the average soil erosion due to water erosion in summer is higher than soil loss in winter and autumn (Schmidt et al. 2019) and precipitation erosivity is the most important factor influencing soil loss (Schmidt et al. 2016). The highest soil erosion rates in both study region occurred when precipitation peaked between June to August (Table 7), which in Mongolia typically for 85–90% of the annual precipitation (Batkhishig 2013).

Table 6 Average soil erosion rate (t ha–1 month–1) in different months (1989–2018)

Study areas	Average: Apr–May		Average: June–Aug		Average: Sep–Oct		Average: Apr–Oct	
	Lowest	Highest	Lowest	Highest	Lowest	Highest	Lowest	Highest
Erdenet	0	0.42	0	4.96	0	0.49	0	2.0
Baganuur	0	0.45	0	4.16	0	0.38	0	1.58

Table 7 Average soil loss rates (t ha^{-1} $month^{-1}$) in different months

Study areas	Average months	Eroded areas (%) of each average months according to different soil loss rates (t ha^{-1} $month^{-1}$)						
		0–0.1	0.1–0.5	0.5–1	1–2	2–3	3–5	> 5
Erdenet	Apr–May	98.98	0.97	0.04	0.01			
	Jun–Aug	75.61	20.32	2.80	0.90	0.21	0.10	0.06
	Sep–Oct	98.21	1.69	0.06	0.04			
	Apr–Oct	90.71	7.82	0.99	0.32	0.07	0.04	0.05
Baganuur	Apr–May	99.28	0.69	0.02	0.01			
	Jun–Aug	81.26	16.01	1.87	0.65	0.13	0.05	0.03
	Sep–Oct	98.08	0.88	1.03	0.01			
	Apr–Oct	93.41	5.69	0.62	0.21	0.04	0.01	0.02

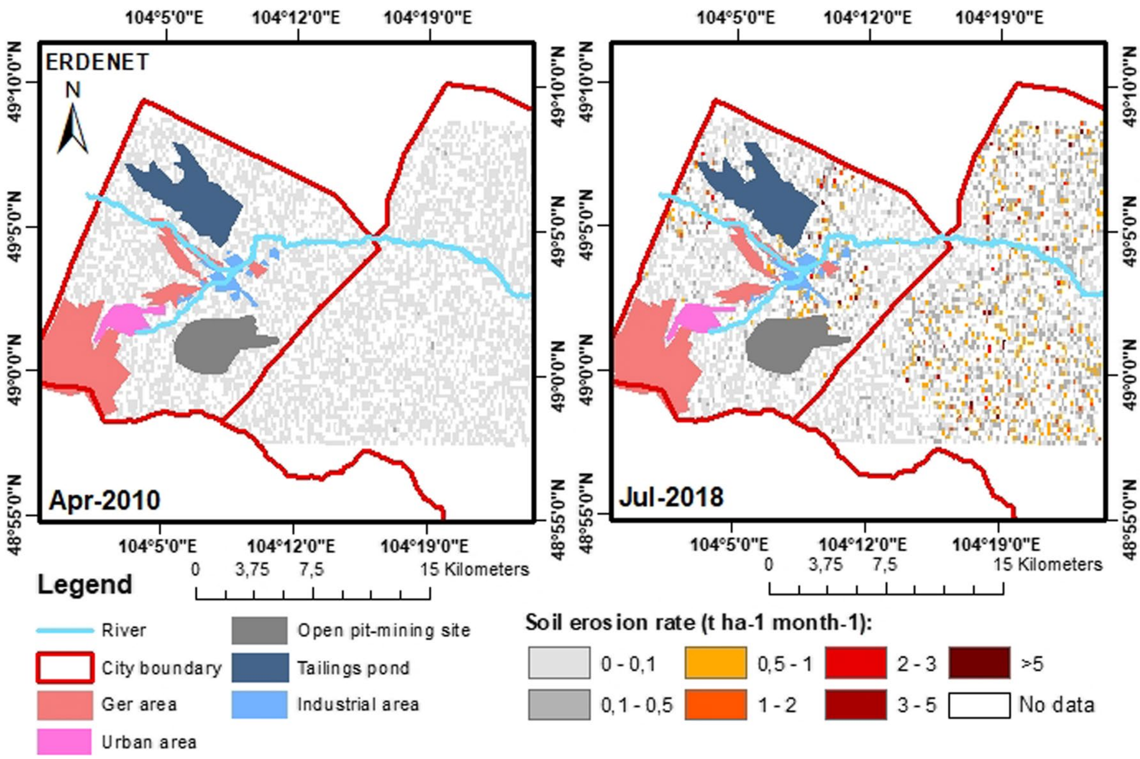

Fig. 7 Spatial patterns of the highest and the lowest soil erosion rate in Erdenet area (The lowest month and year: Apr 2010. The highest month and year: Jul 2018)

Soil erosion rate in Erdenet area

Large parts of the total area (90.71%) experienced only few levels of erosion (0–0.1 t ha^{-1} $month^{-1}$) when considering the entire 30 year observation period. In general, erosion levels increased during the summer months due to higher precipitation. Erosion rates above 2 t ha^{-1} $month^{-1}$ were calculated only for the summer season, with limited areas even experiencing above 5 t ha^{-1} $month^{-1}$. The highest soil erosion rate (8.31 t ha^{-1} $month^{-1}$) was observed in July 2018

Table 8 Soil loss rates distribution by area (t ha^{-1} $month^{-1}$) in the vicinity of different area

Study areas	Areas	Eroded areas (ha) according to different soil loss rates (t ha^{-1} $month^{-1}$)						
		0–0.1	0.1–0.5	0.5–1	1–2	2–3	3–5	> 5
Erdenet	Open-pit mining	1784	370	66	20			
	Tailing pond	1492	501	37	56	23	8	5
	Industrial	673	400	122	25	23	15	0.5
	Ger settlement	1039	144					
	Urban settlement	390	71	20				
Baganuur	Open-pit mining	1977	872	142	31	3	2	
	Industrial	378	164	24	7	1		
	Ger settlement	485	236	38	9	1		
	Urban settlement	503	235	33	10	1	1	

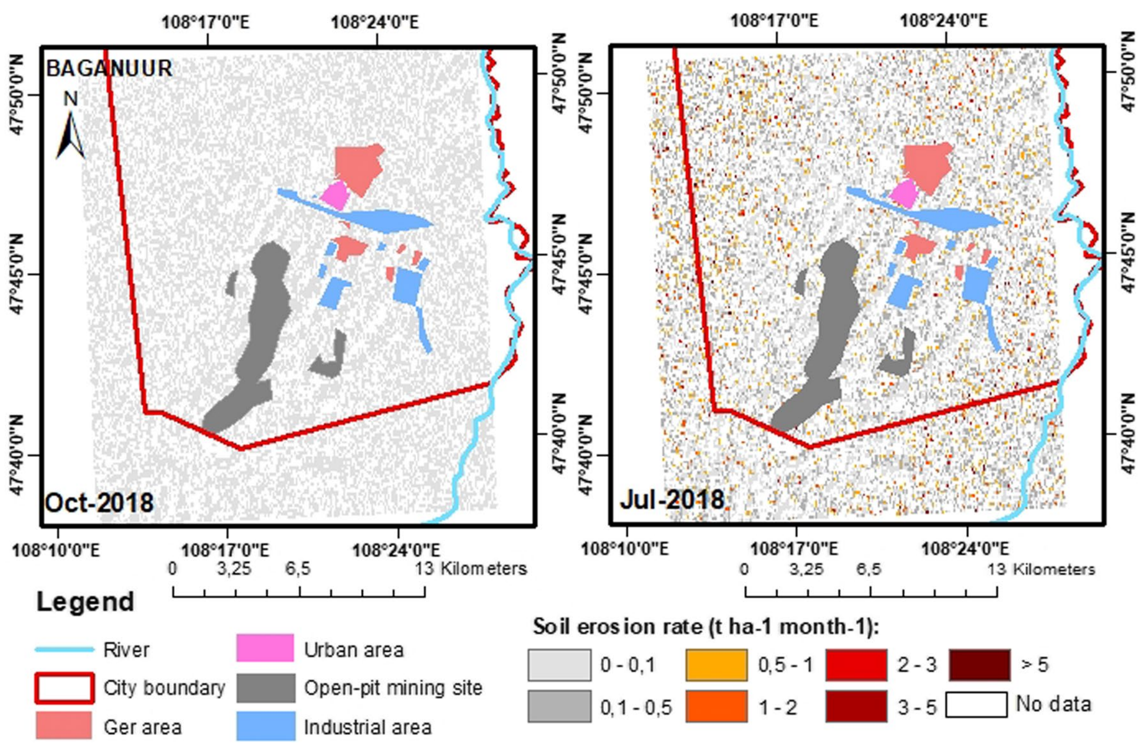

Fig. 8 Spatial patterns of the highest and the lowest soil erosion rate in Baganuur area (The lowest month and year: Apr 2010. The highest month and year: Jul 2018)

and the lowest soil erosion rate (0.05 t ha^{-1} month^{-1}) was calculated for April 2010. These events correlated with the highest rainfall (120.24 mm) in July 2018 and the lowest rainfall (8 mm) in April 2010 of the observation period. The comparison of soil erosion rate in the years with the highest and lowest rainfall in Erdenet is shown in Fig. 7 to illustrate the spatial distribution. Erosion rates were calculated in July 2018 for the approximate area in the vicinity of different land uses such as open-pit mining area, ger area, urban area, tailing pond and industrial area (Table 8). For instance, the calculation showed that a 20 ha area near the open-pit area experienced erosion rates of 1–2 t ha^{-1} month^{-1}. The highest soil erosion rates were found near tailings pond and industrial areas in July 2018.

Soil erosion rate in Baganuur area

The results of the average monthly soil erosion rate were quite similar of those of the Erdenet area, with slightly lower values calculated for Baganuur. This can be explained by the higher rainfall in the Erdenet area.

Table 9 Highest soil loss rates (> 5 t ha^{-1} month^{-1}) and its area

Study area	Soil loss rate (t ha^{-1} month^{-1})	Area (ha)	Soil loss (t month^{-1})	Month-Year
Erdenet	7.88	30	236.4	Jul-2018
	6.65	25	166.25	Aug-2013
	6.23	6	39.738	Jul-1998
	6.12	3	18.36	Jul-1995
Baganuur	9.46	21	198.66	Jul-2018
	8.85	19	168.15	Jul-1998
	5.45	15	81.75	Jul-2013

In the Baganuur area, higher soil erosion rates were observed during June to August, with 0.21% of the total area experiencing erosion of more than 2 t ha^{-1} month^{-1}. The average monthly soil erosion rate was lower in April to May and September to October (Table 7) when a threshold of 2 t ha^{-1} month^{-1} was not exceeded. In July 2018, i.e. the wettest month of the observation period, 0.8% of the total area experienced intensive erosion of more than 2 t ha^{-1} $month^{-1}$. The highest soil loss rate (9.46 t ha^{-1} $month^{-1}$) was found in July 2018 and the lowest soil erosion rate (0.056 t ha^{-1} $month^{-1}$) was found in October 2018, corresponding to the highest amount of rainfall (134.65 mm) in July 2018 and the lowest amount of rainfall (4.46 mm) in October 2018. The comparison of the map with the highest and the lowest soil erosion rates is shown in Fig. 8. In general, a higher erosion rate was found near the open-pit mine and at higher elevations. Erosion rates were calculated in July 2018 for the approximate area considering different land uses (Table 8).

The estimated highest soil loss rates (> 5 t ha^{-1} $month^{-1}$) as well as their area and the amount of eroded soil loss during 1989–2018 in both areas are shown in Table 9. In general, higher soil erosion rates were observed in the Erdenet region than in the Baganuur region. During the study period, the highest erosion in both areas was observed in July 1998, 2013 and July 2018, which is directly related to rainfall.

Discussion and conclusions

This study revealed that in the semi-arid steppe environment of two Mongolia's largest mining sites, the open-cast lignite mine of Baganuur and the open-pit copper–molybdenum mining complex of Erdenet, the spatio-temporal pattern of soil erosion are driven by precipitation pattern and anthropogenic impacts from mining. Some of the highest soil loss rates were found at the extraction sites, but also near mining-related infrastructures such as the tailing pond of Erdenet. The lower soil erosion rates in the vicinity of the open-pit in some respects could be explained by differences in vegetation cover, for instance, a higher vegetation cover found in surrounding areas of the open-pit is explained by lower anthropogenic influences in that area, such as fences. Slightly higher soil loss rates were found in urban and ger settlement areas in Baganuur than in the same settlement areas in Erdenet. This can be attributed to topographic differences between the settlement areas. For example, the urban and ger areas in Baganuur are at a lower elevation and have more opportunities to receive water through precipitation, flooding and snowmelt from the higher elevated areas, and there are several stream channels that run through the settlement (Fig. 1). Soil erosion rates were higher in the Erdenet area as compared to Baganuur, which is mostly due to higher precipitation. The highest monthly erosion rates were 8.31 t ha^{-1} $month^{-1}$ for Erdenet in July 2018, and 9.46 t ha^{-1} $month^{-1}$ for Baganuur in July 2018, which corresponded to the 30-year monthly rainfall maxima in both areas. The exceptionally high rainfall in 2018 can be attributed to El Niño conditions (UNESCAP 2019). In Mongolia, intensive flood events were recorded in July 2018 in several parts of the country, particularly central and northern areas (IFRC 2018). In the light of a trend towards a higher frequency and intensity of extreme precipitation events in the Mongolian steppe zones (Vandandorj et al. 2017), it is likely that such erosion rates will become more frequent in the future. From a soil conservation perspective, it is important to note that apart from steep natural mountain slopes, the highest erosion rates were calculated for the mining sites. Precautionary measures for limiting soil erosion should be considered during mining operation. In the long run, the rehabilitation of abandoned mining sites, and particularly the restoration of surface vegetation, can significantly help in reducing levels. Apart from these specific findings, the results of this study show that a combination of the RUSLE model and a GIS-based approach that integrates ground-based data (in our case, soil texture and soil organic matter to calculate the soil erodibility factor K) and remote sensing-based information (in our case, NDVI as a proxy for the land cover management factor C, the SRTM-DEM for calculating the topographic steepness factor LS, and a global precipitation dataset for deriving the rainfall intensity factor R) can be useful in operationalizing a soil erosion assessment over relatively large areas and long time periods. It is obvious that results should be interpreted with some caution, as all of the above-mentioned ways for quantifying the input parameters of the RUSLE model have their limitations; in our case, the soil erodibility factor was based on limited number of samples, and each of the RS-based datasets has some limitations (e.g. in terms of spatial or horizontal resolution). Nevertheless, the described approach can be a time-saving and cost-effective technique for the operative monitoring and prediction of soil erosion, including the specific situation of mining areas.

Appendix 1

Monthly soil erosion from 1989 to 2018 rate in Erdenet and Baganuur cities.

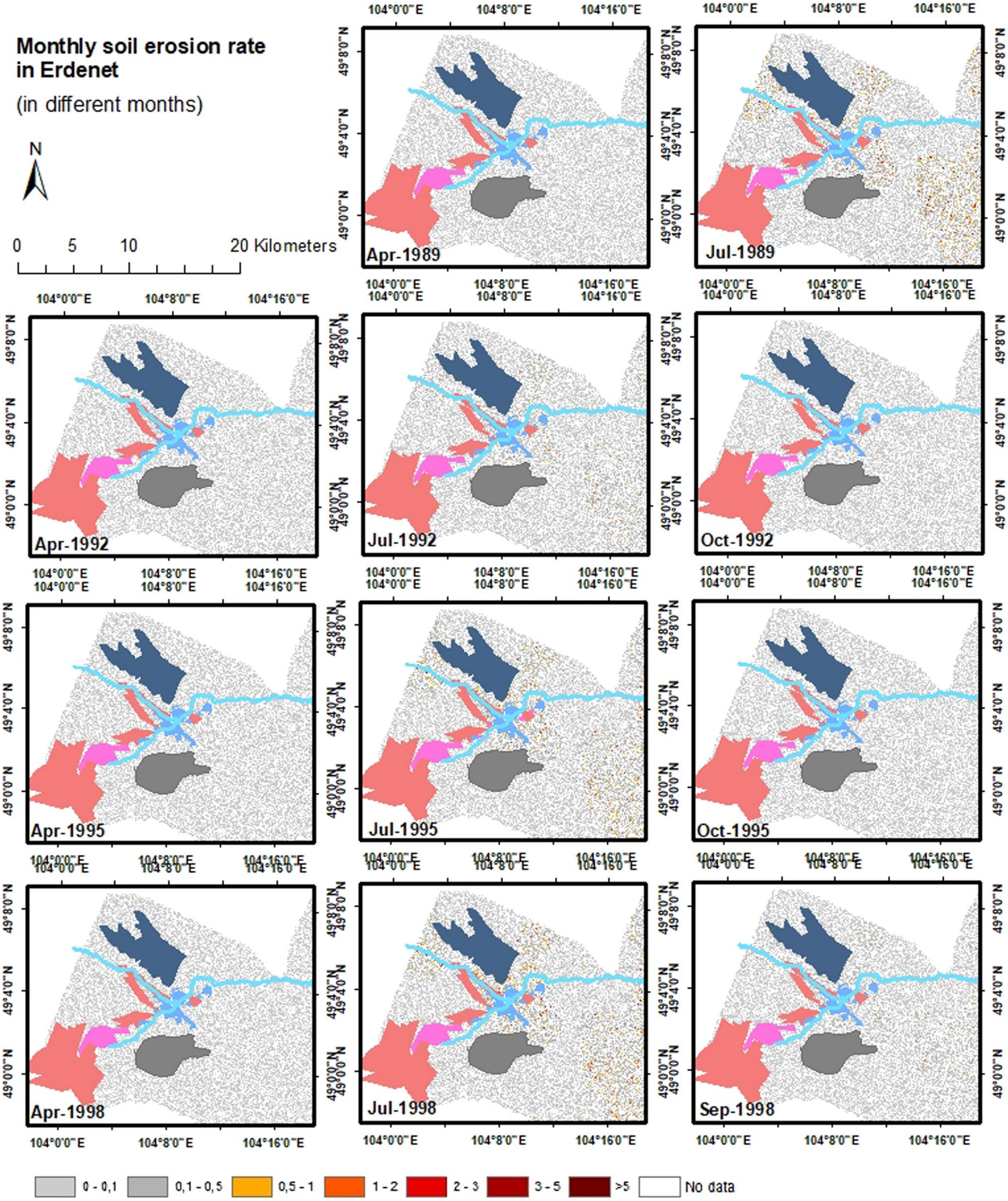

Monthly soil erosion rate in Erdenet
(in different months)
N
0 5 10 20 Kilometers
Apr-1989
Jul-1989
Apr-1992
Jul-1992
Oct-1992
Apr-1995
Jul-1995
Oct-1995
Apr-1998
Jul-1998
Sep-1998
104°0'0"E
104°8'0"E
104°16'0"E
49°8'0"N
49°4'0"N
49°0'0"N
0 - 0,1
0,1 - 0,5
0,5 - 1
1 - 2
2 - 3
3 - 5
>5
No data

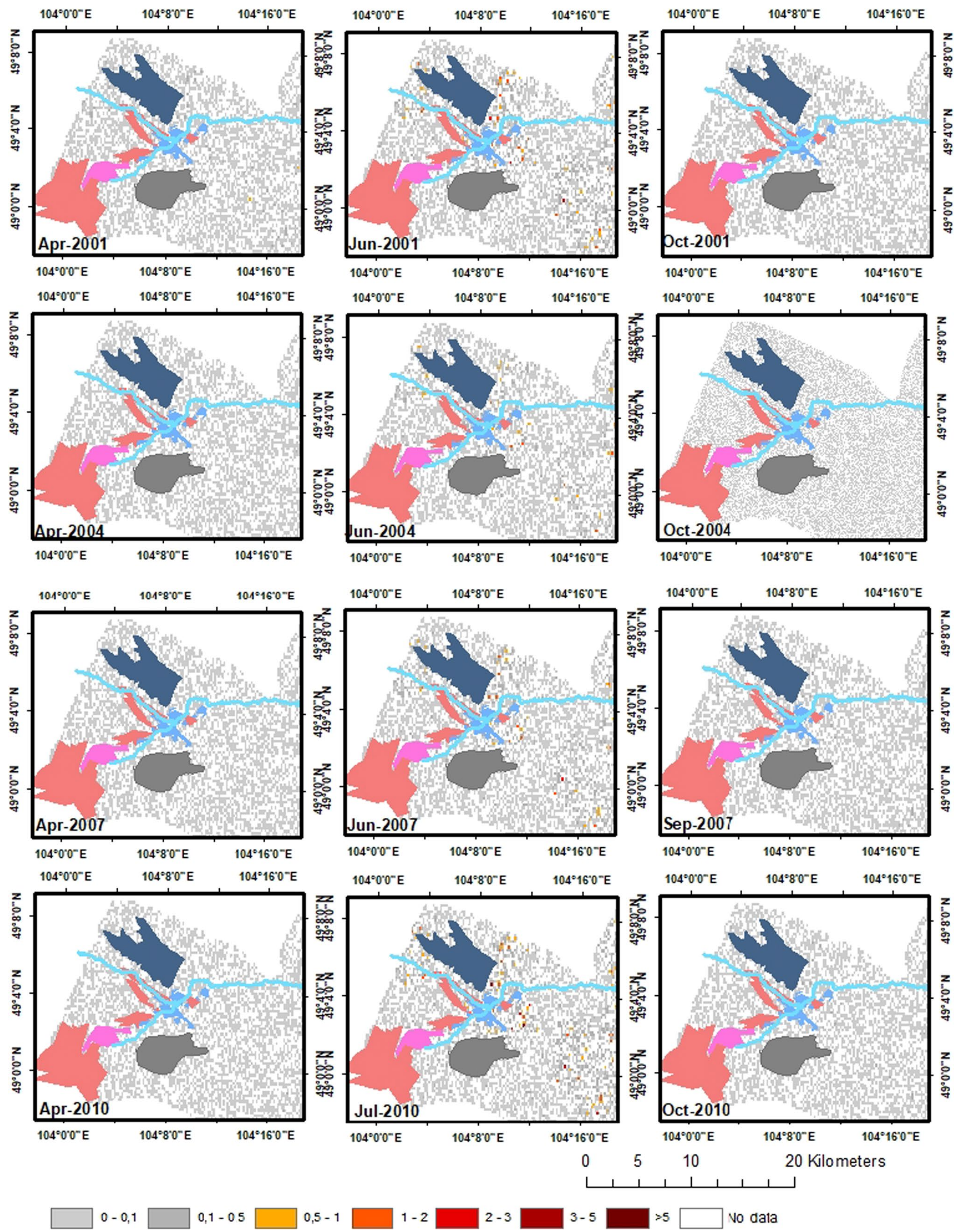
Apr-2001
Jun-2001
Oct-2001
Apr-2004
Jun-2004
Oct-2004
Apr-2007
Jun-2007
Sep-2007
Apr-2010
Jul-2010
Oct-2010
104°0'0"E
104°8'0"E
104°16'0"E
49°8'0"N
49°4'0"N
49°0'0"N
0 5 10 20 Kilometers
0 - 0,1
0,1 - 0 5
0,5 - 1
1 - 2
2 - 3
3 - 5
>5
No data

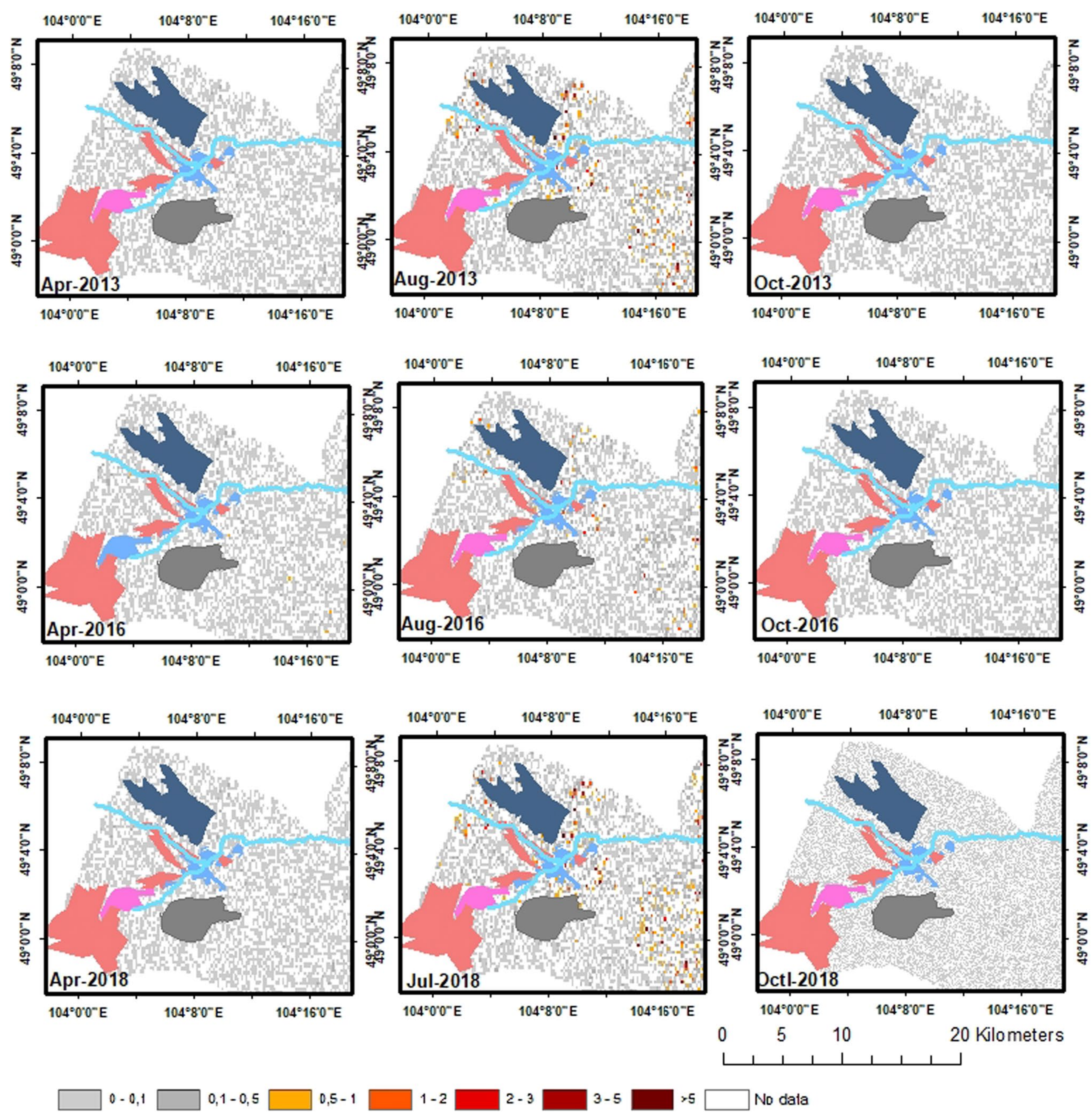
104°0'0"E
104°8'0"E
104°16'0"E
49°8'0"N
49°4'0"N
49°0'0"N
Apr-2013
Aug-2013
Oct-2013
Apr-2016
Aug-2016
Oct-2016
Apr-2018
Jul-2018
Octl-2018
0 5 10 20 Kilometers
0 - 0,1
0,1 - 0,5
0,5 - 1
1 - 2
2 - 3
3 - 5
>5
No data

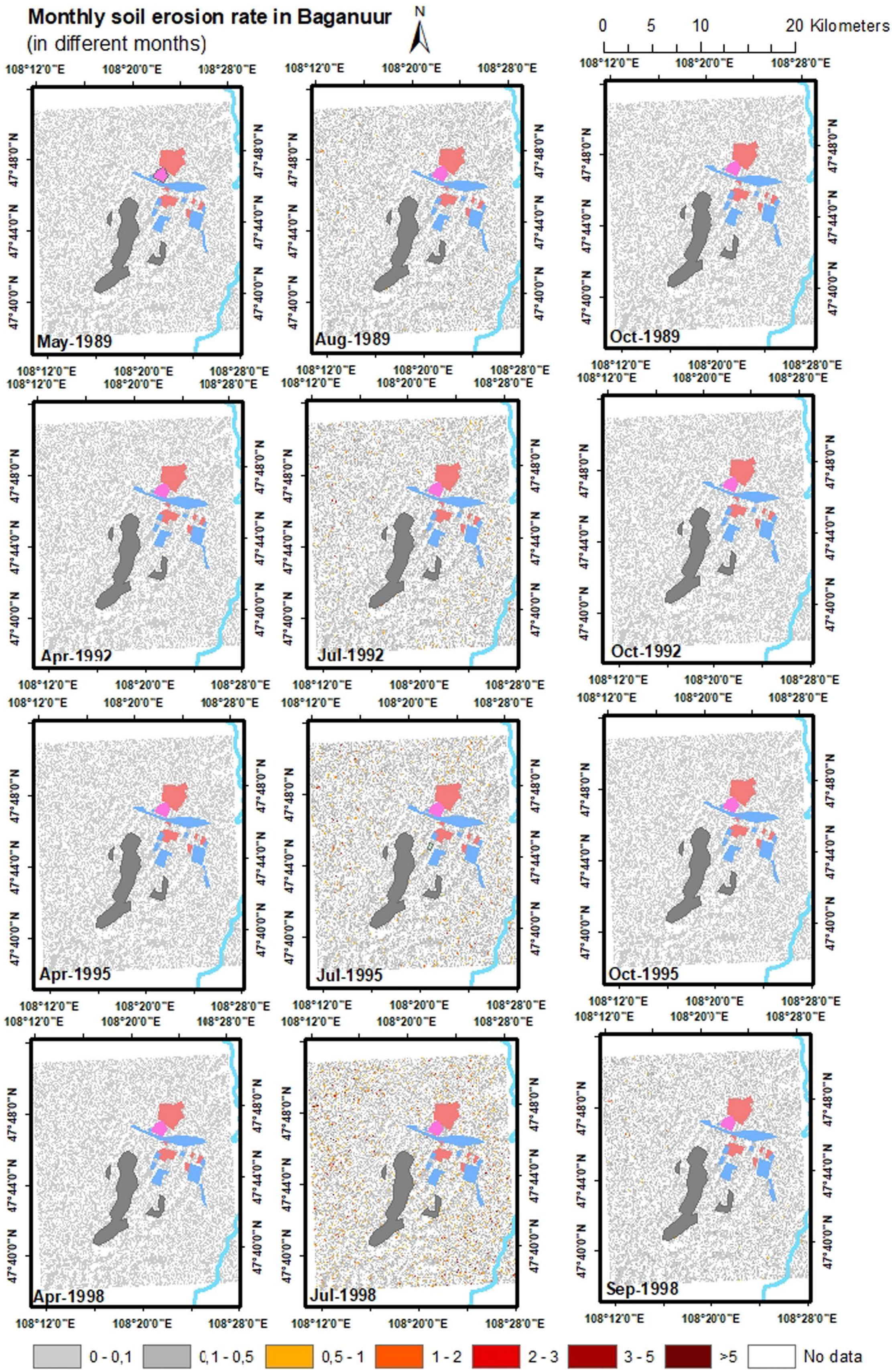
Monthly soil erosion rate in Baganuur
(in different months)
N
0 5 10 20 Kilometers
May-1989
Aug-1989
Oct-1989
Apr-1992
Jul-1992
Oct-1992
Apr-1995
Jul-1995
Oct-1995
Apr-1998
Jul-1998
Sep-1998
108°12'0"E 108°20'0"E 108°28'0"E
47°40'0"N 47°44'0"N 47°48'0"N
0 - 0,1
0,1 - 0,5
0,5 - 1
1 - 2
2 - 3
3 - 5
>5
No data

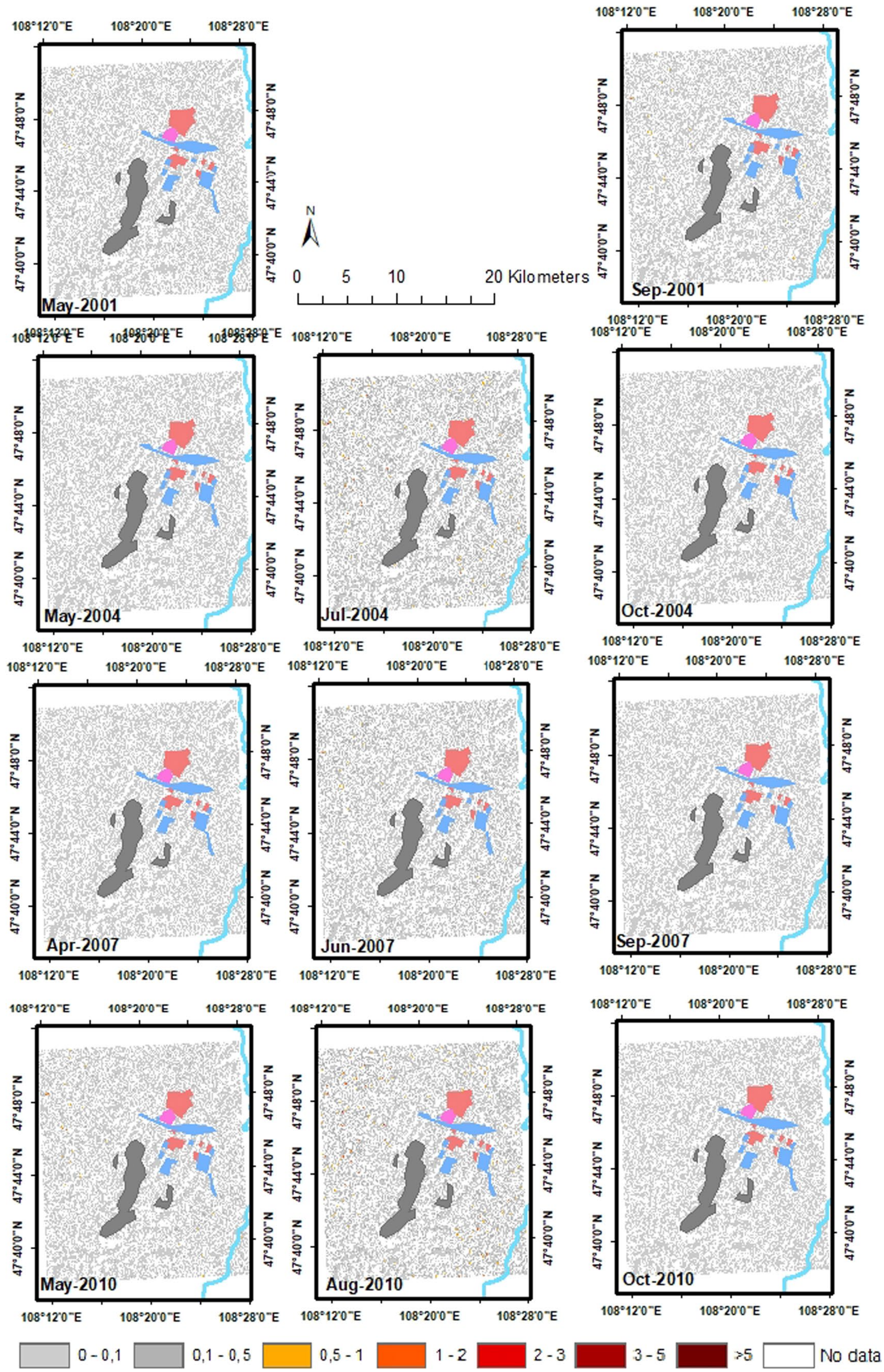
May-2001
Sep-2001
May-2004
Jul-2004
Oct-2004
Apr-2007
Jun-2007
Sep-2007
May-2010
Aug-2010
Oct-2010
108°12'0"E
108°20'0"E
108°28'0"E
47°40'0"N
47°44'0"N
47°48'0"N
N
0 5 10 20 Kilometers
0 - 0,1
0,1 - 0,5
0,5 - 1
1 - 2
2 - 3
3 - 5
>5
No data

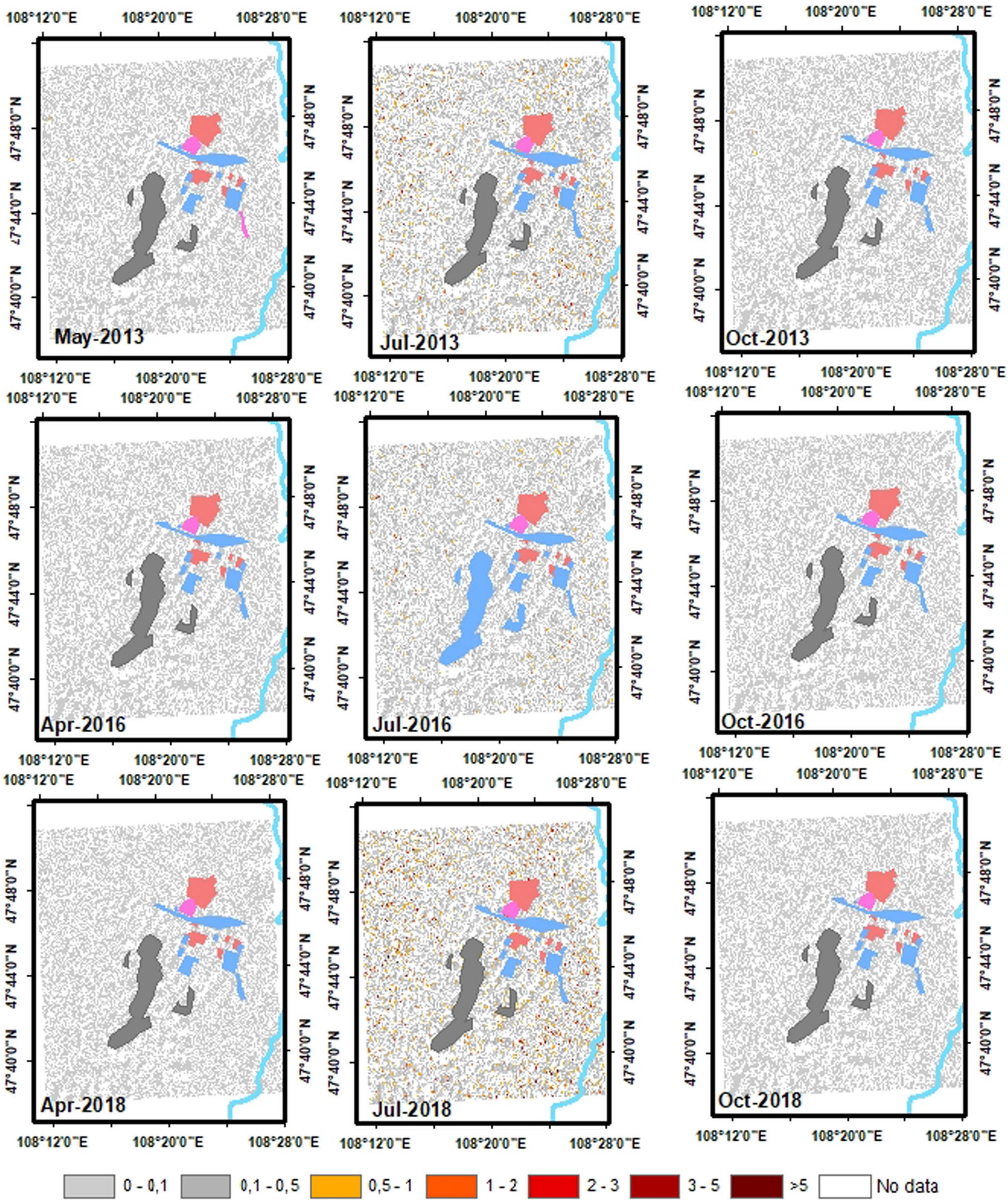
108°12'0"E
108°20'0"E
108°28'0"E
47°40'0"N
47°44'0"N
47°48'0"N
May-2013
Jul-2013
Oct-2013
Apr-2016
Jul-2016
Oct-2016
Apr-2018
Jul-2018
Oct-2018
0 - 0,1
0,1 - 0,5
0,5 - 1
1 - 2
2 - 3
3 - 5
>5
No data

Acknowledgements The authors would like to express their appreciation to the German Academic Exchange Service (DAAD) for awarding a scholarship for the PhD sandwich program of RWTH Aachen University, Germany and the German-Mongolian Institute for Resources and Technology (GMIT), Mongolia. Also, great appreciation to Mr. Malte Giesenow who organized administrative and other related work of the project.

Funding Open Access funding enabled and organized by Projekt DEAL. This work was funded by Deutscher Akademischer Austauschdienst.

Data availability The authors confirm that the data supporting the findings of this study are available within the article.

Declarations

Conflict of interest The authors have not disclosed any competing interests.

References

Abatzoglou J, Dobrowski S, Parks S, Hegewisch P (2018) TerraClimate a high-resolution global dataset of monthly climate and climatic water balance from 1958–2015. Sci Data 5:17019. https://doi.org/10.1038/sdata.2017.191

Alewell C, Borrelli P, Meusburger K, Panagos P (2019) Using the USLE: chances, challenges and limitations of soil erosion modelling. Int Soil Water Conse 7(3):203–225. https://doi.org/10.1016/j.iswcr.2019.05.004

Baatarzorig T, Galindev R, Maisonnave H (2018) Effects of ups and downs of the Mongolian mining sector. J Environ Dev Econ 23(5):527–542. https://doi.org/10.1017/S1355770X18000153

Bahrawi AJ, Elhag M, Aldhebiani AY, Galal HK, Hegazy A, Alghailani E (2016) Soil erosion estimation using remote sensing techniques in Wadi Yalamlam basin, Saudi Arabia. Adv Mater Sci Eng. https://doi.org/10.1155/2016/9585962

Batbayar G, Pfeiffer M, von Tümpling W, Kappas M, Karthe D (2017) Chemical water quality gradients of the sub catchments of the Mongolian Selenga River basin. J of Environ Monit Assess 189:420. https://doi.org/10.1007/s10661-017-6123-z

Batkhishig O (2013) Human impact and land. Degradation in Mongolia, Chapter 12. In: Chen et al. (eds) the volume dry land East Asia: land dynamics amid social and climate change. Ecosystem Science and application. The Higher Education Press, pp 265–282

Batkhishig O, Lehmkuhl F, Oyunbat P, Samdandorj M (2019). Soil erosion study using radionuclide techniques in southern Mongolia, Orog lake area. EST-2019 International conference

Batmunkh I (2021) Environmental Issues in the Mining Sector of Mongolia. Environl Prot 12(6):415–427. https://doi.org/10.4236/jep.2021.126025

Battogtokh B, Lee JM, Woo N (2013) Contamination of water and soil by the Erdenet copper–molybdenum mine in Mongolia. Environ Earth Sci 71:3363–3374. https://doi.org/10.1007/s12665-013-2727-y

Boussaadi M, Mouzai L (2021) Vegetation cover effects on sediment concentration and overland flow under artificial rainfall intensity. Jovan Cvijic SASA 71(2):135–150. https://doi.org/10.2298/IJGI2102135B

Chonokhuu S, Batbold Ch, Chuluunpurev B, Battsengel E, Dorjsuren B, Byambaa B (2019) Contamination and health risk assessment of heavy metals in the soil of major cities in Mongolia. Environ Res Public Health 16(14):2552. https://doi.org/10.3390/ijerph16142552

ClimateData (2020) Worldwide climate data source. https://en.climate-data.org/. Accessed 1999–2019

Dagys K, Heijman WJM, Dries L, Agipar B (2020) The mining sector boom in Mongolia: did it cause the Dutch disease? J of Post-Communist Econ 32(5):607–642. https://doi.org/10.1080/14631377.2019.1689002

Darbalaeva D, Mikheeva A, Zhamyanova Y (2020) The socio-economic consequences of the desertification processes in Mongolia. E3S Web Conf 164:11001, TPACEE-2019. https://doi.org/10.1051/e3sconf/202016411001

Davaasambuu N (2018) Study report on mining and infrastructure development, further planning: National Development Agency of Mongolia. http://regional.nda.gov.mn/backend/f/df3mbmdVjA.pdf. Accessed July 2018

Durigon VL, Carvalho DF, Antunes MAH, Oliveira PTS, Fernandos MM (2014) NDVI time series for monitoring RUSLE cover management factor in a tropical watershed. Remote Sens. https://doi.org/10.1080/01431161.2013.871081

Duulatov E, Pham QB, Alamanov S (2021) Assessing the potential of soil erosion in Kyrgyzstan based on RUSLE, integrated with remote sensing. Environ Earth Sci 80:658. https://doi.org/10.1007/s12665-021-09943-6

Eckert S, Husler F, Liniger H, Hodel E (2015) Trend analysis of MODIS NDVI time series for detecting land degradation and regeneration in Mongolia. J Arid Environ 113:16–28. https://doi.org/10.1016/j.jaridenv.2014.09.001

Farrington JD (2005) The impact of mining activities on Mongolia's Protected areas: a status report with policy recommendations. Integr Environ Asses 1(3):283–289. https://doi.org/10.1897/2004-008R.1

Han J, Dai H, Gu Z (2021) Sandstorms and desertification in Mongolia, an example of future climate events: a review. Environ Chem Lett 19:4063–4073. https://doi.org/10.1007/s10311-021-01285-w

Hartwig M, Schäffer M, Theuring P, Avlyush S, Rode M, Borchardt D (2016) Cause–effect–response chains linking source identification of eroded sediments, loss of aquatic ecosystem integrity and management options in a steppe river catchment (Kharaa, Mongolia). Environ Earth Sci 75:855. https://doi.org/10.1007/s12665-015-5092-1

Hateffard F, Mohammed S, Alsafadi K, Enaruvbe GO, Heidari A, Abdo HG, Rodrigo-Comino J (2021) CMIP5 climate projections and RUSLE-based soil erosion assessment in the central part of Iran. Sci Rep. https://doi.org/10.1038/s41598-021-86618-z

Heiri O, Lotter AF, Lemcke G (2001) Loss on ignition as a method for estimating organic and carbonate content in sediments: reproducibility and comparability of results. J Paleolimnol 25:11–110

Hofmann J, Tuul D, Bazarradnaa E (2016) Agriculture in Mongolia Under Pressure of Agronomic Nutrient Imbalances and Food

Security Demands: A Case Study of Stakeholder Participation for Future Nutrient and Water Resource Management. In: Borchardt D, Bogardi J, Ibisch R (eds) Integrated Water Resources Management: Concept, Research and Implementation, Springer, Cham. 471–514. https://doi.org/10.1007/978-3-319-25071-7_19

Huang X, Lin L, Ding S, Tian Z, Zhu X, Wu K, Zhao Y (2022) Characteristics of Soil Erodibility K Value and Its Influencing Factors in the Changyan Watershed, Southwest Hubei. China Land 11(1):134. https://doi.org/10.3390/land11010134

IFRC International Federation of Red Cross and Red Crescent Societies (2018) Emergency plan of action Mongolia: Flash floods. https://www.ifrc.org/. Accessed July 2018

Jarsjö J, Chalov SR, Pietroń J, Alekseenko AV, Thorslund J (2017) Patterns of soil contamination, erosion and river loading of metals in a gold mining region of northern Mongolia. Reg Environ Change 17:1991–2005. https://doi.org/10.1007/s10113-017-1169-6

Karthe D, Kasimov NS, Chalov SR, Shinkareva G (2014) Integrating multi-scale data for the assessment of water availability and quality in the Kharaa-Orkhon-Selenga river system. Geogr Environ Sustain 7(3):65–86. https://doi.org/10.24057/2071-9388-2014-7-3-40-49

Karthe D, Chalov S, Moreydo V, Pashkina M, Romanchenko A, Batbayar G, Kalugin A, Westphal K, Malsy M, Flörke M (2017) Assessment and prediction of runoff, water and sediment quality in the Selenga river basin aided by a web-based Geoservice. Water Resour 44(3):399–416. https://doi.org/10.1134/S0097807817030113

Kato H, Onda Y, Tanaka Y (2010) Using ^{137}CS and $^{210}Pb_{ex}$ measurements to estimate soil redistribution rates on semi-arid grassland in Mongolia. Geomorphology 114(4):508–519. https://doi.org/10.1016/j.geomorph.2009.08.009

Kaus A, Schäffer M, Karthe D, Büttner O, von Tümpling W, Borchardt D (2017) Regional patterns of heavy metal concentrations in water, sediment and five consumed fish species of the Kharaa River basin, Mongolia. Reg Environ Change 17:2023–2037. https://doi.org/10.1007/s10113-016-0969-4

Kayet N, Pathek K, Chakrabarty A, Sahoo S (2018) Evaluation of soil loss estimation using the RUSLE model and SCS–CN method in hillslope mining areas. Int Soil Water Conserv Res 6(1):31–42. https://doi.org/10.1016/j.iswcr.2017.11.002

Kebede YS, Endalamaw NT, Sinshaw BG, Atinkut HB (2021) Modeling soil erosion using RUSLE and GIS at watershed level in the upper beles, Ethiopia. Environ Challenges 2:100009. https://doi.org/10.1016/j.envc.2020.100009

Khishigjargal B, Khishigsuren N, Dolgormaa Sh, Ya B (2015) Biological rehabilitation in the degraded land, a case study of Shariingol soum of Selenge aimag in Mongolia. Mongolian J Agric Sci 15(2):106–112. https://doi.org/10.5564/mjas.v15i2.555

Kim SH, Yu T, Kashima K (2017) The history of palaeoflood and palaeoclimate recorded in the flood deposits of the Kherlen river Mongolia. Quatern Int. https://doi.org/10.1016/j.quaint.2017.05.026

Knippertz M (2005) Analysis of the rehabilitation potential of copper mining areas in Zambia and Mongolia. Doctoral thesis, RWTH Aachen, 40

Köppen, W. Das geographische System der Klimate, 1–44 (Gebrüder Borntraeger: Berlin, Germany, 1936).

Kosheleva NE, Kasimov NS, Timofeev IV (2018) Potentially toxic elements in urban soil catenas of W-Mo (Zamamensk, Russia) and Cu-Mo (Erdenet, Mongolia) mining areas. J Soils Sediments 18:2318–2334. https://doi.org/10.1007/s11368-017-1897-8

Kulimushi LC, Choudhari P, Mubalama LK, Banswe GT (2021) GIS and remote sensing based assessment of soil erosion risk using RUSLE model in South Kivu province, eastern, Democratic Republic of Congo. Geomat Nat Haz Risk 12(1):961–987. https://doi.org/10.1080/19475705.2021.1906759

Lee J, Lee S, Hong J, Lee D, Bae JH, Yang JE, Kim J, Lim KJ (2021) Evaluation of rainfall erosivity factor estimation using machine and deep learning models. Water 13(3):382. https://doi.org/10.3390/w13030382

Lehmkuhl F, Batkhishig O (2003) Degradation and Desertification in Mongolia. Petermanns Geographical communications 147(5), 48–49 http://publications.rwth-aachen.de/record/151933. Accessed 2002

Liang X, Li P, Wang J, Sh CFK, Togtokh Ch, Ochir A, Davaasuren D (2021) Research progress of Desertification and its prevention in Mongolia. Sustainability 13(12):6861. https://doi.org/10.3390/su13126861

Maqsoom A, Aslam B, Hassan U, Kazmi ZA, Sodangi M, Tufail RF, Farooq D (2020) Geospatial assessment of soil erosion intensity and sediment yield using the Revised Universal Soil Loss Equation (RUSLE) model. IRPRS Int J Geo-Inf 9(6):356. https://doi.org/10.3390/ijgi9060356

Mineral Resources and Petroleum Authority of Mongolia (MRPAM) (2020): Mineral Resources and Petroleum Statistics 2020/01. Online at: https://mrpam.gov.mn/public/pages/165/2020.01.stat.report.eng.pdf. Accessed Jan 2020

Mukul M, Srivastava V, Jade S, Mukul M (2017) Uncertainties in the Shuttle Radar Topography Mission (SRTM) Heights: Insights from the Indian Himalaya and Peninsula. Sci Rep 7:41672. https://doi.org/10.1038/srep41672

Munkhtsengel B, Ohara M, Gerel O, Dandar S, Tsuchiya N (2006) Preliminary study of formation mechanism of the Erdenetiin ovoo porpHyry copper–molybdenum deposit and environmental effects of Erdenet mine, northern Mongolia. AIP Conf Proc 833:204. https://doi.org/10.1063/1.2207106

Nottebaum V, Walk J, Knippertz M, Karthe D, Batbayar G, Pötter S, Lehmkuhl F (2020) Arsenic distribution and pathway scenarios for sediments and water in a peri-urban Mongolian small-scale coal mining area (Nalaikh, Ulaanbaatar District). Environ Sci Pollut Res 27:5845–5863. https://doi.org/10.1007/s11356-019-07271-8

NSO National Statistical Office (2018) A report of social and economic development measuring status. https://www.1212.mn/. Accessed Jan 2018

Onda Y, Kato H, Tanaka Y, Tsujimura M, Davaa G, Oyunbaatar D (2007) Analysis of runoff generation and soil erosion processes by using environmental radionuclides in semiarid areas of Mongolia. J Hydrol 333:124–132. https://doi.org/10.1016/j.jhydrol.2006.07.030

Otgochuluu Ch, Bold-Erdene R (2015) The potential fo methane gas development in Mongolia. Erina report 127

Ouadja A, Benfetta H, Porto P (2021) Mapping potential soil erosion using RUSLE, Remote Sensing, and GIS: a case study in the watershed of Oued El Ardjem Northwest Algeria. Arab J of Geosci 14:1945. https://doi.org/10.1007/s12517-021-07992-6

Panagos P, Borrelli P, Meusburger K, Alewell Ch, Lugato E, Montanarella L (2015) Estimating the soil erosion cover-management factor at the European scale. Land Use Policy 48:38–50. https://doi.org/10.1016/j.landusepol.2015.05.021

Park J, Kwon E, Chung E, Kim E, Kim H, Battogtokh B, Woo NC (2020) Environmental Sustainability of Open-pit Coal mining practices at Baganuur. Mongolia Sustain 12(1):248. https://doi.org/10.3390/su12010248

Parveen R, Kumar U (2012) Integrated Approach of Universal Soil loss equation and GIS for Soil loss risk assessment in upper South Koel Basin, Jharkhand. J Geogr Inf Syst 4:588–596. https://doi.org/10.4236/jgis.2012.46061

Priess J, Schweitzer C, Batkhishig O, Koschitzki T, Wurbs D (2015) Impacts of land-use dynamics on erosion risks and water management in Northern Mongolia. Environ Earth Sci 73:697–708. https://doi.org/10.1007/s12665-014-3380-9

Renard KG, Freimund JR (1994) Using monthly precipitation data to estimate the R-factor in the revised USLE. J Hydrol 157:287–306

Renard KG, Foster GR, Weesies GA, Porter JP (1991) RUSLE: revised universal soil loss equation. Soil Water Conserv. https://www.tucson.ars.ag.gov/unit/publications/pdffiles/775.pdf

Schmidt S, Alewell C, Panagos P, Meusburger K (2016) Regionalization of monthly rainfall erosivity patterns in Switzerland. Hydrol Earth Syst Sc 20:4359–4373. https://doi.org/10.5194/hess-20-4359-2016

Schmidt S, Alewell Ch, Meusburger K (2019) Monthly RUSLE soil erosion risk of Swiss grasslands. J Maps 15(2):247–256. https://doi.org/10.1080/17445647.2019.1585980

Schoderer M, Karthe D, Dombrowsky I, Dell'Angelo J (2021) Hydrosocial dynamics of miningscapes: Obstacles to implementing water protection legislation in Mongolia. J Environ Manage 292:112767. https://doi.org/10.1016/j.jenvman.2021.112767

Schulte EE, Hopkins BG (1996) Estimation of soil organic matter by weight 3 organic matter (LOI) loss-on-ignition. pp.21–31. In: Magdoff FR, Tabatabai MA, Hanlon Jr EA (eds) Soil organic matter: analysis and interpretation. Soil Sci. Soc. Am., Madison, WI.

Schwab GO, Frevert RK, Edminster TW, Barnes K (1981) Soil water conservation engineering, 3rd edn. Wiley.

Shojaei S, Kalantari Z, Rodrigo-Comino J (2020) Prediction of factors affecting activation of soil erosion by mathematical modeling at pedon scale under laboratory conditions. Sci Rep 10:20163. https://doi.org/10.1038/s41598-020-76926-1

Solongo Ts, Fukushi K, Altansukh O, Takahashi Yo, Akehi A, Baasansuren G, Ariuntungalag Yu, Enkhjin O, Davaajargal B, Davaadorj D, Hosebe N (2018) Distribution and chemical speciation of molybdenum in river and pond sediments affected by mining activity in Erdenet city, Mongolia. Minerals 8(7):288. https://doi.org/10.3390/min8070288

Tessema YM, Jasinska J, Yadeta LM, Switoniak M, Puchalka R, Gebregeorgis EG (2020) Soil loss estimation for conservation planning in the Welme watershed of the Genale Dawa basin. Ethiopia Agron 10(6):777. https://doi.org/10.3390/agronomy10060777

Theuring P, Collins AL, Rode M (2015) Source identification of fine-grained suspended sediment in the Kharaa River basin, northern Mongolia. Sci Total Environ 526:77–87. https://doi.org/10.1016/j.scitotenv.2015.03.134

Timofeev IV, Kosheleva NE, Kasimov NS, Gunin PD, Sandag E (2016) Geochemical transformation of soil cover in copper–molybdenum mining areas (Erdenet, Mongolia). J Soils Sediments 16:1225–1237. https://doi.org/10.1007/s11368-015-1126-2

Turmunkh B (2020) Foreign Direct Investment and investment environment on mining sector in Mongolia. Conf EEA C, Section 6. 50-57. https://doi.org/10.29013/EJEMS-19-2-50-57

UNCCD United Nations Convention to Combat Desertification (2018). Investing in land degradation neutrality making the case–Mongolia. https://www.unccd.int/. Accessed Jan 2018

UNESCAP United Nations Economic and Social Commission for Asia and the pacific (2019) 2018/2019 El Niño Asia-Pacific impact outlook for March to April 2019 https://www.unescap.org/. Accessed March to April 2019

USDA United States Department of Agriculture (2017) Soil texture analysis. https://www.usda.gov/. Accessed July 2017

USGS the U.S Geological Survey's web site, Earth Explorer data portal of The United States of America. https://earthexplorer.usgs.gov/. Accessed 23 Sept 2014

Vandandorj S, Munkhjargal E, Boldgiv B, Gantsetseg B (2017) Changes in event number and duration of rain types over Mongolia from 1981 to 2014. Environ Earth Sci 76:70. https://doi.org/10.1007/s12665-016-6380-0

Wang J, Wei H, Cheng K, Ochir A, Davaasuren D, Li P, Chan FKS, Nasanbat E (2020) Spatio-Temporal Pattern of Land Degradation from 1990 to 2015 in Mongolia. Environ Dev 34:100497. https://doi.org/10.1016/j.envdev.2020.100497

WorldClim (Version 2.1) Historical climate data https://www.worldclim.org/. Accessed January to December, 1986–2018

Worsham L, Markewitz D, Nibbelink NP, West LT (2012) A Comparison of three field sampling methods to estimate soil carbon content. Forest Sci 58(5):513–522. https://doi.org/10.5849/forsci.11-084